BACKGROUND AND PROJECT OBJECTIVES

The presence of hydrogen stratification in a Nuclear Power Plant (NPP) containment following a postulated severe accident is a safety concern. Pockets of hydrogen of high concentration could lead to a deflagration or detonation, which might damage safety equipment necessary for safety functions and even challenge the containment's structural integrity. The analysis of various thermal-hydraulic processes leading to the stratification of hydrogen during its release and the potential destabilization or break-up of the hydrogen layer by the operation of engineered systems e.g. coolers, sprays, and passive autocatalytic recombiners (PAR) are very complex to predict. The complexity arises from the fact that a large number of interrelated processes should be taken in consideration for the analysis, for example convective flows produced by jets and plumes (with positive or negative buoyancy), diffusion, transport induced by density or pressure differences, condensation occurring on relatively cold walls or initiated by activation of safety systems, and finally re-evaporation or condensation. Additionally, the performance of active (e.g. spray, active cooler) or passive safety systems (e.g. PAR, passive cooler) would depend on the specific safety component design and as well on the thermal-hydraulic conditions in the containment and therefore would vary during the evolution of a postulated severe accident.

Advanced Lumped Parameter (LP) and Computational Fluid Dynamic (CFD) codes are valuable tools for analyzing nuclear power plant containment behavior during postulated design and beyond-design-basis accidents. The computational tools are continuously validated and improved and take advantage of the continuing increase in computing power and in the accumulated knowledge in understanding thermal-hydraulic phenomena. Experimental data needed for code validation have to be obtained, preferably from large scale tests, minimizing the impact of scaling distortions in the assessment of the code models. Nonetheless, tests with comparable initial and boundary conditions in facilities with different geometrical scales and compartmentalization allow for insights on the phenomenology to be associated with investigated accident scenarios, and to identify the effects which could be facility dependent and therefore not to be expected in real plant containment.

At present, the extent of code validation, code user training and experience are limiting factors for the reactor safety analysis. One of the hindrances in the process of assessment and validation of computational tools is the lack of adequate experimental data with the required spatial and time resolution. In addition, the available data do not cover the required broad range of phenomena and scenarios anticipated in various reactor containments under all the postulated accident conditions.

The EURATOM co-financed ERCOSAM project and the ROSATOM co-financed SAMARA project have been conducted in parallel during the period 2010-2014, in the framework of a cooperation agreement, to investigate the containment thermal-hydraulics of current and future LWRs for severe accident management.

The ERCOSAM-SAMARA projects had two main objectives. The first was to establish, for a severe accident sequence chosen from existing plant calculations and representative of a LOCA in a LWR,

the strength of hydrogen stratification that can be established during part of the transient period, starting from the late blowdown until the end of hydrogen release from the reactor vessel into the containment. The second was to determine whether this stratification, once established, can be broken down by the operation of SAM devices: sprays, coolers and heat release by PARs.

WORK PERFORMED

Based on the collection of existing LOCA calculations for various nuclear power plant (NPPs) designs, the reference scenario which has been selected is a Small Break LOCA in a PWR with dry containment, which generally constitutes the highest contribution to the core damage frequency. The considered NPPs characteristics have been used to define the containment of a generic NPP of about 1000 MW_{th} power. The generic containment has been determined by scaling down from PWR 1300 configuration, considering the ratio between the generic and the PWR 1300 containment volumes. Validation of the generic containment, scaled down from real plant, was performed through new calculations of the selected scenarios with the corresponding scaled source terms on the generic containment. Comparisons of the generic calculation results with the reference plants show similar conditions in terms of predicted pressure and temperature and also of global and local steam and hydrogen quantities such as mass and concentration.

The source terms (steam, hydrogen) have been averaged to obtain constant mass and enthalpy flow rates during the steam and hydrogen injection phases.

The approach to define the tests in the various facilities, where hydrogen was replaced by helium, was to follow the simplified accident scenarios with constant steam and helium injection mass flow rates, by considering four distinct and consecutive phases (Figure 1).

Phase 1 addressed the blowdown, characterized by steam release from the break during the postulated LOCA and the containment pressurization. Phase 2 simulated the phase of the accident following the blowdown involving core damage leading to the release of hydrogen and steam into the containment. Phases 3 simulated the phases of the accident when no more steam and hydrogen was released from the reactor coolant system into the containment. In Phase 4, a component (spray, cooler or heater) was activated to study its effect on the gas species (helium, steam, air) evolution in the containment [1].

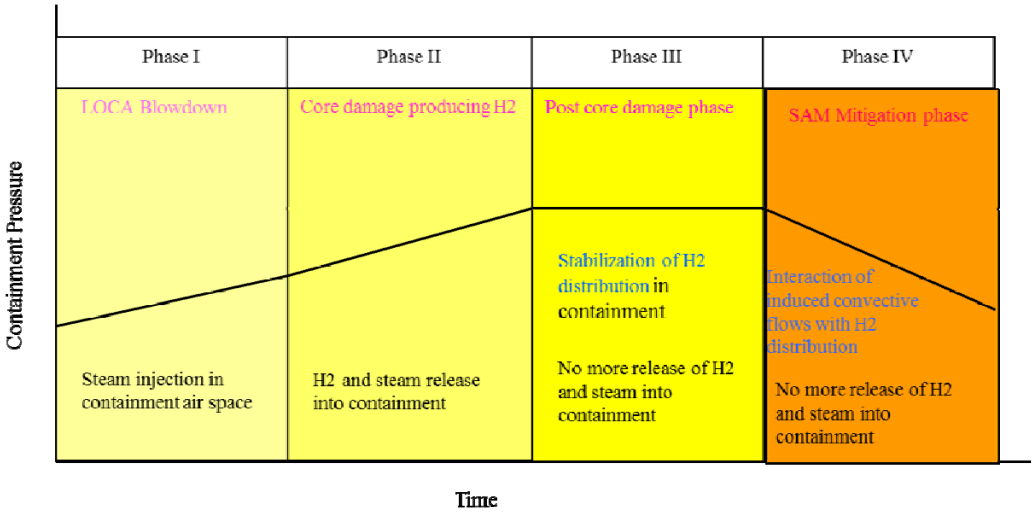

Figure 1: Idealized test scenarios.

The test initial and boundary conditions in Phases 1, 2 and 3 were determined, with the target to reach at the end of Phase 3 the total containment pressure and the helium volume fraction in the upper dome similar to those obtained in the generic containment analysis: ~2.5 bar; ~12% helium molar fraction. Due to the difference in the steam/helium release characteristics in the experimental facilities (through injection pipes in a large volume, which result in a given gas composition at the pipe exit) and the releases expected from the steam generator compartment (large opening in the steam generator compartment, which allow a mixing of the release fluid with the compartment gas mixture) of the generic containment, refined calculations applied to the facility geometries and preliminary tests (shake-down tests which aim to develop the appropriate preconditioning protocols) were carried out to identify the appropriate test initial conditions (air/steam mixture temperature, pressure and composition) at the start of Phase 1.

EXPERIMENTAL FACILITIES

The facilities are different in their main dimensions and compartmentalization. The TOSQAN (IRSN, France) facility [2] (Figure 2) is a single compartmental vessel with a volume of 7 m^3, with a diameter of 1.5 m and height of 4.8 m.

The MISTRA (CEA, France) facility [3] (Figure 3) has a multi-compartment geometry and a total volume of 97.6 m^3, an inner diameter of 4.25 m and a height of 7.38 m.

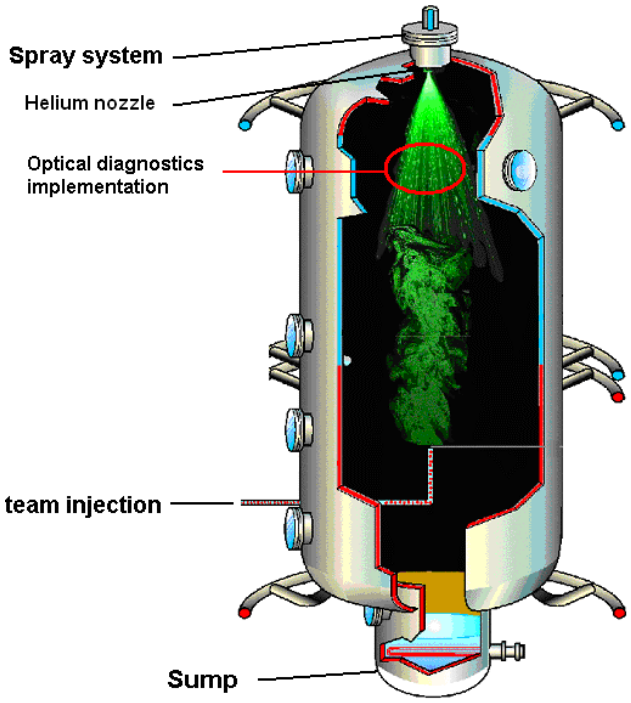

Figure 2: Schematics of the TOSQAN facility [2]. Facility main characteristics: Volume = 7m^3, Diameter 1.5m, Height 4.8m.

Figure 3: Schematics of the MISTRA facility [3]. Facility characteristics: Main injection lines (lower centered (1), lower off centered (2), upper off centered (3) for steam and incondensable gas) Volume = 99.5m^3, Diameter = 3.8m, Height = 7.4m, Compartmented volume.

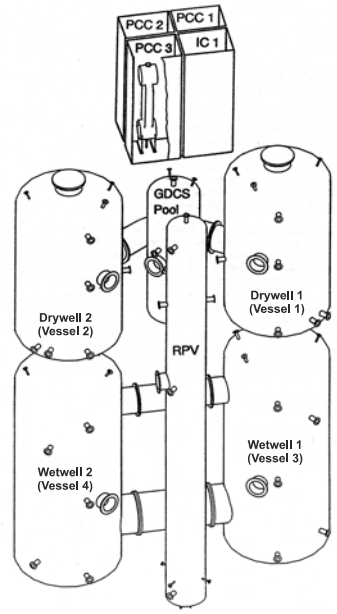

Figure 4: Schematics of the PANDA facility [4], [5]. Facility characteristics: Volume of the upper drywell vessels = 2 x 90m^3, Diameter = 4m, Height = 8m.

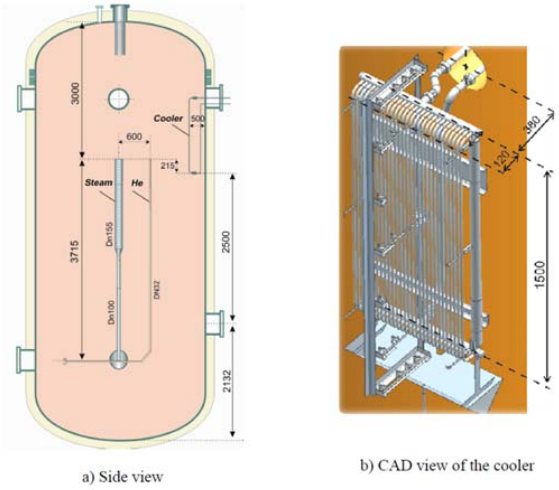

a) Side view

b) CAD view of the cooler

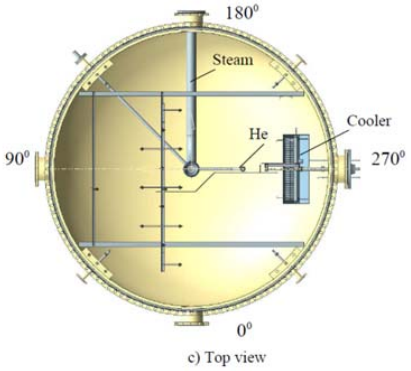

c) Top view

Figure 5: Schematic of the SPOT facility [6]. Facility characteristics: volume =59 m^3, Diameter = 3.2 m, Height = 9 m.

PANDA (PSI, Switzerland) is a multi-compartment facility [4], [5] (Figure 4) with a total volume (six vessels) of approximately 515 m3 and an overall height of 25 m and vessels with inner diameter of 4 m.

The SPOT ("JSC Afrikantov OKB", Russia) facility [6] (Figure 5) is a single compartment vessel with a total volume of 59 m^3, internal diameter of 3.2 m and height 9 m.

HYMIX CONCEPTUAL FACILITY

A conceptual facility [7] named HYMIX (IBRAE-RAN, Russia) has been defined with a volume of 3181 m , inner diameter of 14 m and height 23 m. The HYMIX analytical tests addressed the effect of activation of spray (K1) (Figure 6) and cooler (K2) (Figure 7).

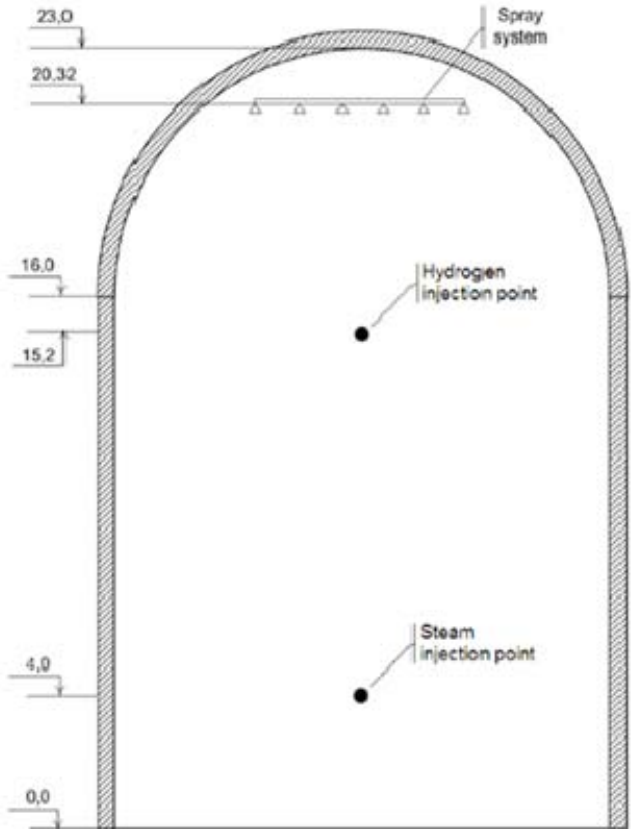

Figure 6: Cross-section of K1 HYMIX configuration [7].

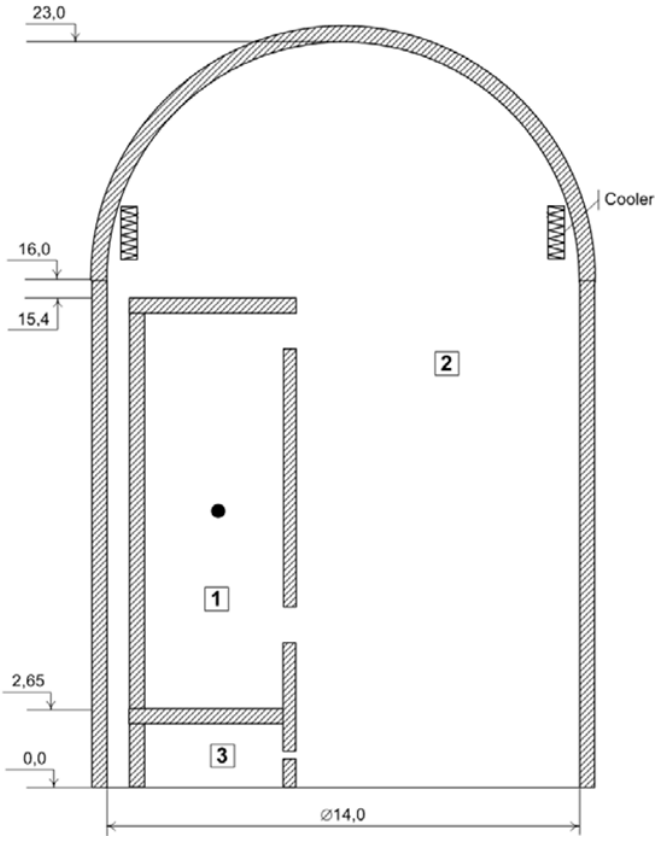

Figure 7: Cross-section of K2 HYMIX configuration [7].

RESEARCH INVESTIGATIONS PERFORMED

Table 1 shows the experiments which have been performed. Despite the fact that several aspects of the tests performed in each facility are different, an effort has been made to define the Phase 4 for selected tests with comparable initial and boundary conditions. The remaining tests have been defined to address parameters which provide a broader understanding on the basic phenomenology and in some cases the effect of component designs. For instance the same hollow cone spray nozzle and spray injection flow rate has been used in MERCO_1 and PE1 tests, so that it was possible to investigate the effect on the gas species evolution of spray activation for two types of multi-compartments (PANDA: two large/empty interconnected volumes; MISTRA: one large volume with inner compartment). The PE2 test was performed using a full cone nozzle, and spray water injection conditions as for the PE1 test. Comparing these two PANDA tests allowed for study of the effect of a spray induced flow pattern, which can be more uniformly distributed in the case of the hollow cone nozzle. The T114, T115, T116 tests have been performed with a full cone nozzle and for different initial and boundary conditions and allowed the observation of the phenomenology evolution in a smaller scale facility. The K1 spray analytical test has been defined considering geometrical similarities with the PE2 test, for example, HYMIX configured as an empty containment compartment, and leaving an empty volume between the spray nozzle exit and the top of the containment. Moreover, full cone spray nozzles have been considered in K1 on a ring in the

containment periphery. The analysis of spray tests (e.g. MERCO_1, PE2, etc.) allowed for assessment of the code and refinement of the models, while the code to code K1 analysis allowed for insight on the code predictions at the HYMIX scale (e.g. intermediate scale toward a LWR real containment).

Table 1: ERCOSAM-SAMARA experiments

Facility	Test	SAM device
Experiments		
TOSQAN	T114	Full cone spray
	T115	Full cone spray
	T116	Full cone spray
PANDA	PE1	Hollow cone spray
	PE2	Full cone spray
	PE3	Cooler
	PE4	Heater
	PE5	Cooler
MISTRA	MERCO_0	No SAM activation
	MERCO_1	Hollow cone spray
	MERCO_2	Cooler
	MERCO_3	1 heater
	MERCO_4	2 heater
SPOT	S1	Cooler
	S2	Cooler
Analytical tests		
HYMIX	K1	Spray
	K2	Cooler

The Phase 4 for the tests performed with a heater, MERCO_3, MERCO_4 and PE4, have been defined considering heater power curves resembling the energy which could be released by a PAR. The metallic cases (box type geometry) for the heater elements used in MISTRA and PANDA allowed similar flow paths, for example a horizontal opening at the inlet (vertical flow path into the heater) and vertical opening at the exit (horizontal flow path at the exit of the heater). In the PE4 test,

the heater element was installed at an intermediate elevation near the interconnecting pipe elevation. The MERCO_3 test was performed with a single heater installed in the periphery of the facility, in the region of the internal compartment exit elevation. The MERCO_4 test was performed with two heater elements installed at the same elevation and radial location as in MERCO_3 but a different circumferential angle. By comparing the three tests, it was possible to observe the induced heat source convective flow for different facility geometries (PE4, MERCO_3) and moreover the flow pattern created by two heat sources (MERCO_4).

The PE3, PE5, MERCO_2, S1, S2 tests and the K2 analytical test have been performed by activating a heat sink in Phase 4, for example cooler devices or, in the case of MERCO_2, a condenser. The initial vessel wall and fluid condition for PE5 and S2 tests were defined in such a way as to avoid wall condensation and therefore to observe specifically the effect from the cooler operation. These two tests permitted observation of the effect of cooler design for two different facility scales. The combined cooler and wall condensation effects have been investigated in PE3 test.

The controlled wall condensation has been investigated in MERCO_2 with the middle condenser acting as heat sink. The S1 and S2 tests have been defined with the cooler and the source release in the middle region of the containment as for PE3 and P5 tests. The S1 test has been defined with the same scenarios as PE3. In the S2 test the cooler has been activated during the helium release phase to observe the cooler effect on the helium stratification build-up during the helium release and on the overall mixing (after the helium release phase has been completed).

The K2 analytical test has been defined with the design of the coolers the same as those used in the S1 and S2 tests and considering the volume to cooler-power scaling ratio. Moreover the source (steam, hydrogen) release in K2 analytical test has been located inside a room/compartment and the test allow to observe hydrogen distribution in a multi-compartment including accumulation in dead end volumes.

All the organizations participating in the ERCOSAM-SAMARA projects contributed, via code simulations, to the definition and analysis of TOSQAN, SPOT, MISTRA and PANDA experiments and the HYMIX analytical tests. For the simulations, the following codes have been used: Lumped parameter codes ASTEC, COCOSYS, TONUS_LP, KUPOL-MT; the CFD-type codes GOTHIC and GASFLOW; the commercial CFD codes FLUENT and CFX; and the open source CFD code, OpenFOAM. Some tests have been analyzed using the same computational tool by various Organizations. The analytical activities associated with the test definition included planning calculations, and the analyses of the tests included pre-test and post-test calculations.

Moreover, the preliminary calculations (before the actual planning calculations), performed to verify that the gas mixture conditions in PANDA, MISTRA, TOSQAN and SPOT facilities would be representative of the conditions in the generic containment, revealed that due to the facility simplified geometries (which cannot represent the mixing in the break room) a strong steam stratification was to be expected during Phase 1 which would then remain for the following Phases 2 and 3, and this would have caused a major distortion in the mixture stratification in the facilities with

respect to the generic containment, for which approximately uniform steam/air mixture was expected over the containment height. The approach to overcome to this distortion was to define for the scenario an additional phase, called Phase 0 (Figure 8), which would create a more uniform steam/air mixture composition in the facilities, and therefore be more representative of the generic containment conditions.

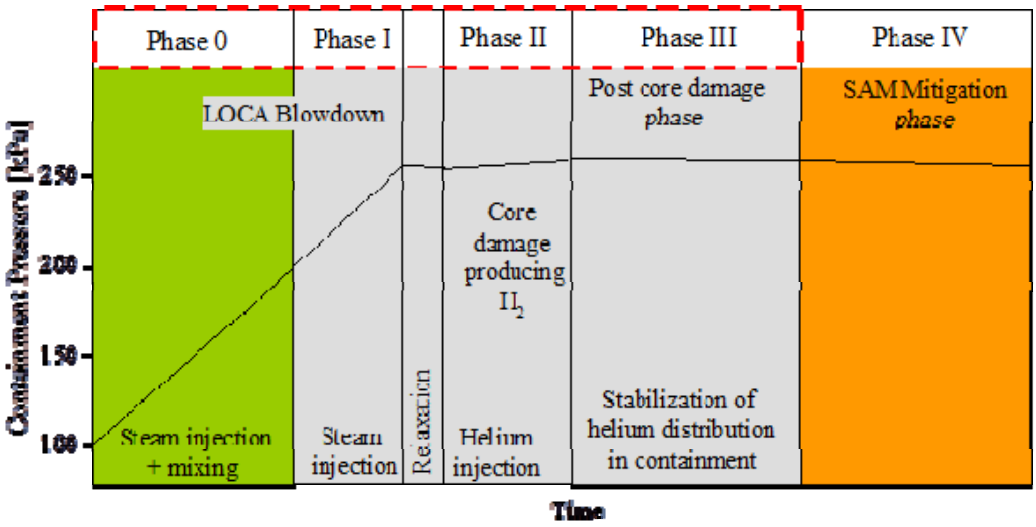

Figure 8: Example of modified accident scenarios with inclusion of Phase 0 [32].

Planning calculations have been performed for all phases of the tests to study the effects of various parameters on the gas distributions, and the interaction of the components (cooler, heater, spray) with the stratified ambient conditions. Additionally these studies provided indications on the optimal positions for the key measurements.

The pre-test and post-test analyses have been carried out to assess the code capability to simulate the tests. For the pre-test analysis, the test specifications (nominal values) have been used, while the actual test conditions were used for the post-test analysis.

HIGHLIGHTS OF THE EXPERIMENTS AND ANALYSIS

The TOSQAN [8], MISTRA [9-12], SPOT [13-15], PANDA [16-20] tests have been carried out according to test protocols developed through preliminary tests (shake-down tests) and considering the findings obtained with the planning calculations. It should be pointed out that the test protocols to reach the target conditions were defined considering the facility characteristics: auxiliary systems and location of injection and venting lines and therefore are different in the various facilities. Moreover, the facility designs such as compartment type, volume/surface ratio, and presence of localized heat sinks, had their own effect on the evolution of test phenomenology. Protocols have been defined also for the HYMIX analytical tests [21].

The global phenomena taking place in Phases 1 (release of steam), 2 (release of helium) and 3 (stabilization) are: containment pressurization (TOSQAN: 2.2- 2.8 bar [22] (Figure 9); MISTRA:

2.56 bar [23-27] (Figure 10); SPOT: 2.5 bar [28] (Figure 11); PANDA: 2.5 bar [29] (Figure 12), [30-33]), and gas mixture stratification build-up (helium in the upper layer of the vessel, e.g. TOSQAN: up to 100% (Figure 13); MISTRA: 9.5% (Figure 14); SPOT: 12% (Figure 15); PANDA: 12-14% (Figure 16).

Moreover, thermal stratification was observed in the vessel wall and gas space. The thermal stratification was related to the injection conditions, (such as injection exit elevation), to the facility characteristics (presence of concentrated heat sinks, inter-compartment flow transport) and to the condensation and re-evaporation phenomena, which were taking place in some of the tests due to the specified initial and boundary conditions.

The global phenomena which took place in Phase 4 (activation of spray, cooler or heater), were containment depressurization (cooler and spray), as well as gas atmosphere mixing (cooler, spray, heat source).

For instance, with respect to the tests performed with spray activation, the PE1 (with hollow cone nozzle) and PE2 (with full cone nozzle) tests had similar depressurization rates; the containment pressure decreased from 2.5 bar to 1.5 bar in about 2000 s. Nonetheless in the PE1 test, the phenomenology associated with gas species evolution was more complex, due to the initial higher gas/wall thermal stratification in the vessel. This further affected the condensation and re-evaporation phenomena as well as the inter-compartment flow transport. As result, in the PE1 test (Figures 17 and 18) the helium-rich layer was broken more quickly than in PE2 (Figures 19 and 20). In MERCO-1 test (hollow cone), the pressure decreased from 2.56 bar to 1.5 bar in about 1500 s and in a shorter time the helium-rich layer was broken. In the T115 test the pressure decreases to 1.7 bar in about 5000 s. In the T114 and T116 tests the re-evaporation of sump prevailed on the condensation of steam on the injected spray droplets and as one consequence the facility pressure increased.

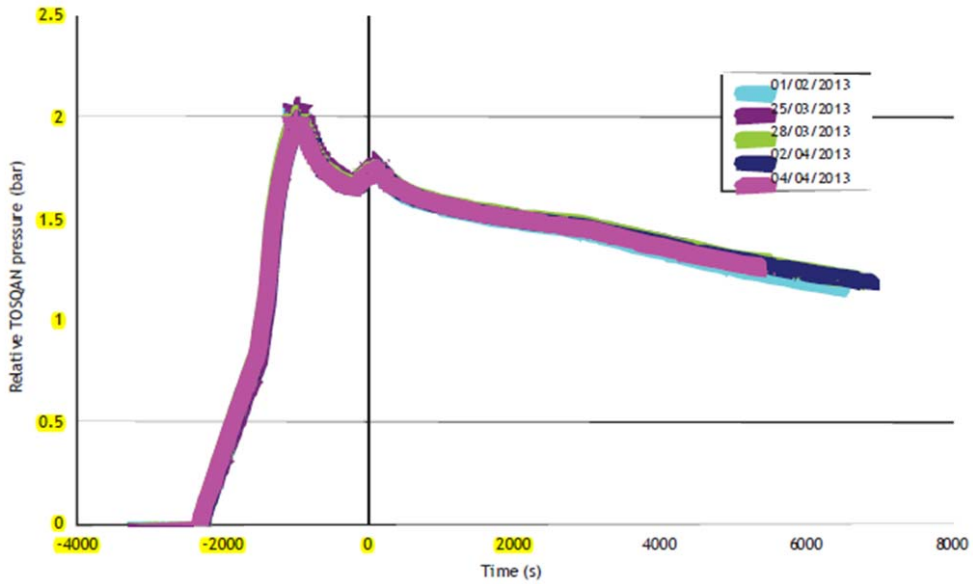

Figure 9: Temporal evolution of the pressure for the different T115 tests [22].

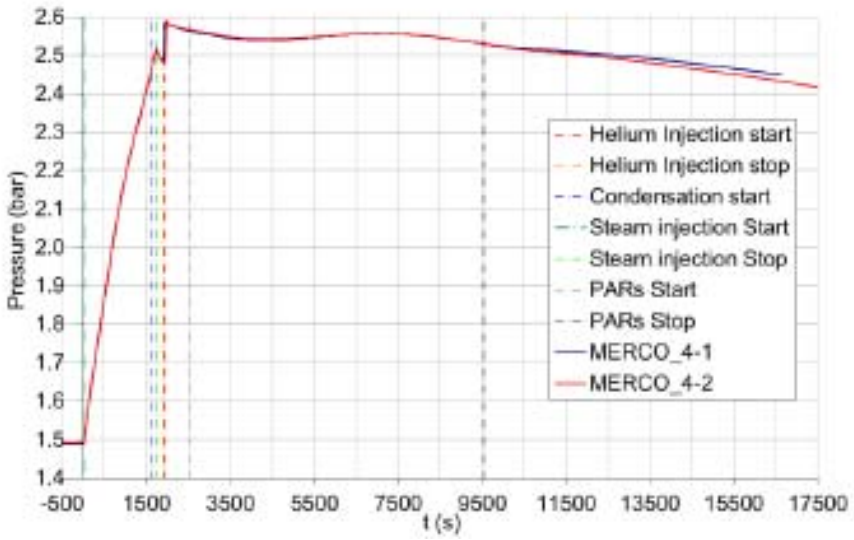

Figure 10: Reproducibility of the pressure evolution – MERCO_4 test [26].

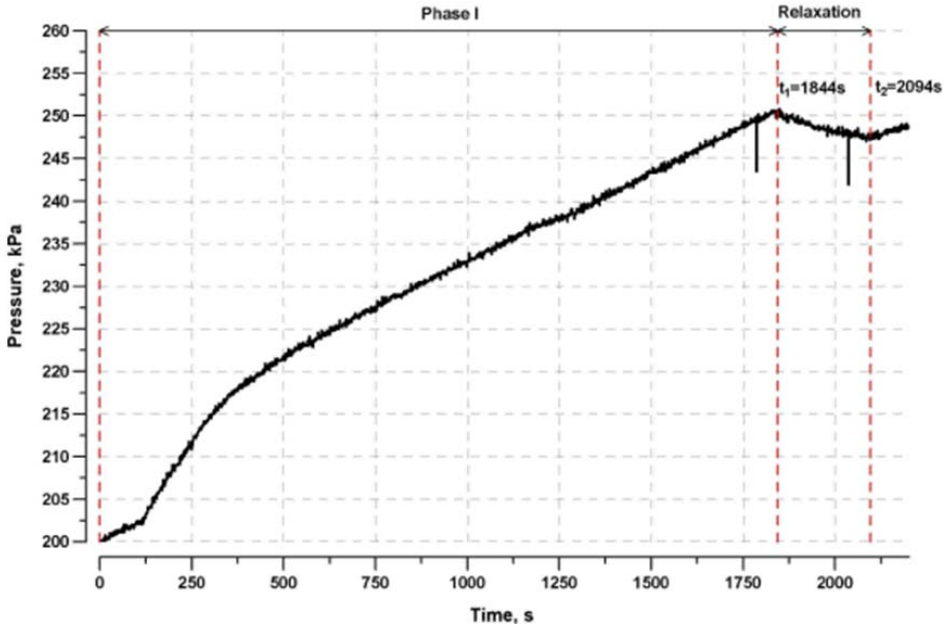

Figure 11: Pressure evolution during Phase 1 and relaxation Phase in SPOT [28].

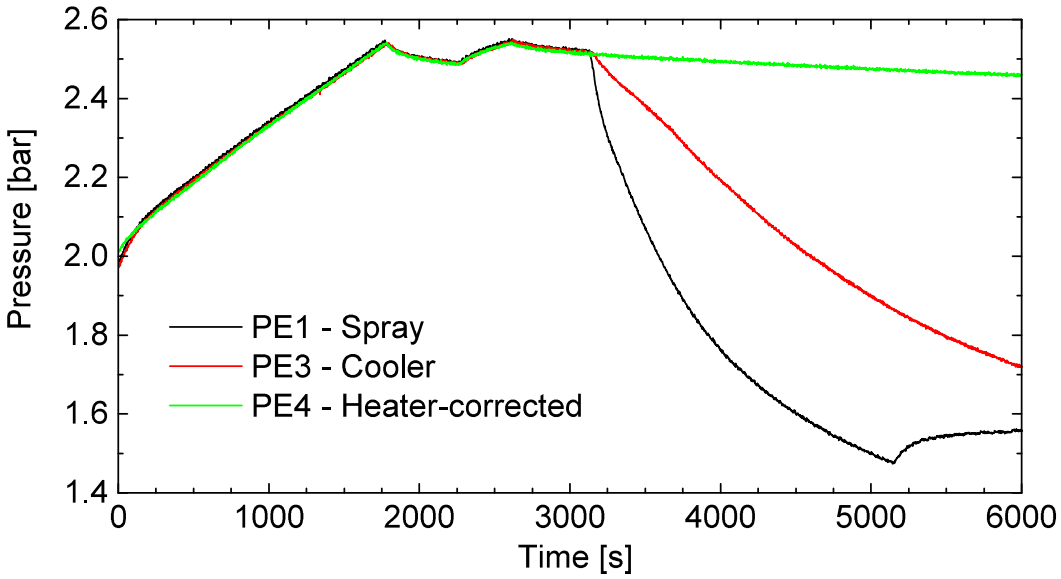

Figure 12: Pressure evolution in PANDA vessels during

Phase 1 to 4 of PE1, PE3 and PE5 [29-32] tests (with wall condensation).

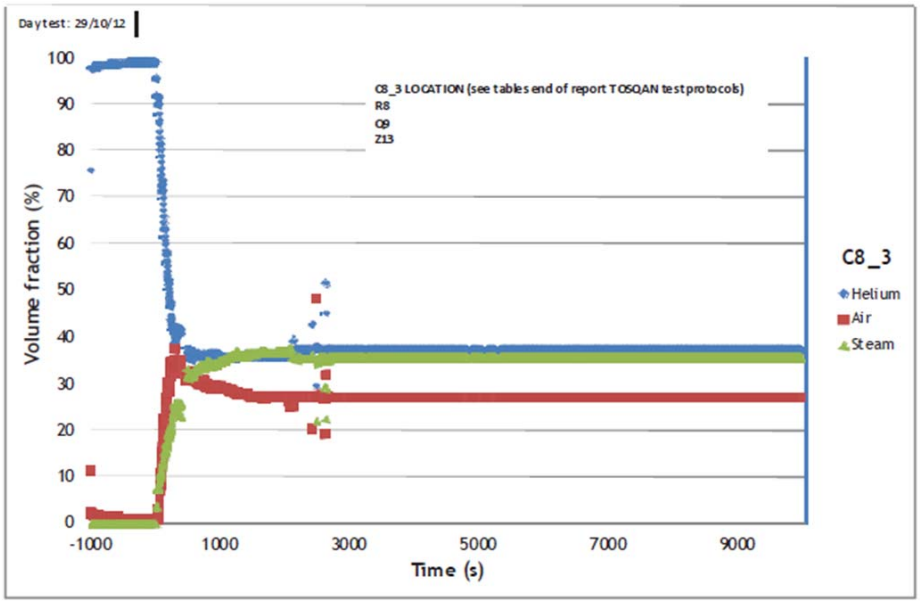

Figure 13: Volume fraction of helium, steam and air

on position C8_3 (R8, Q9, Z13) in T114 test [22].

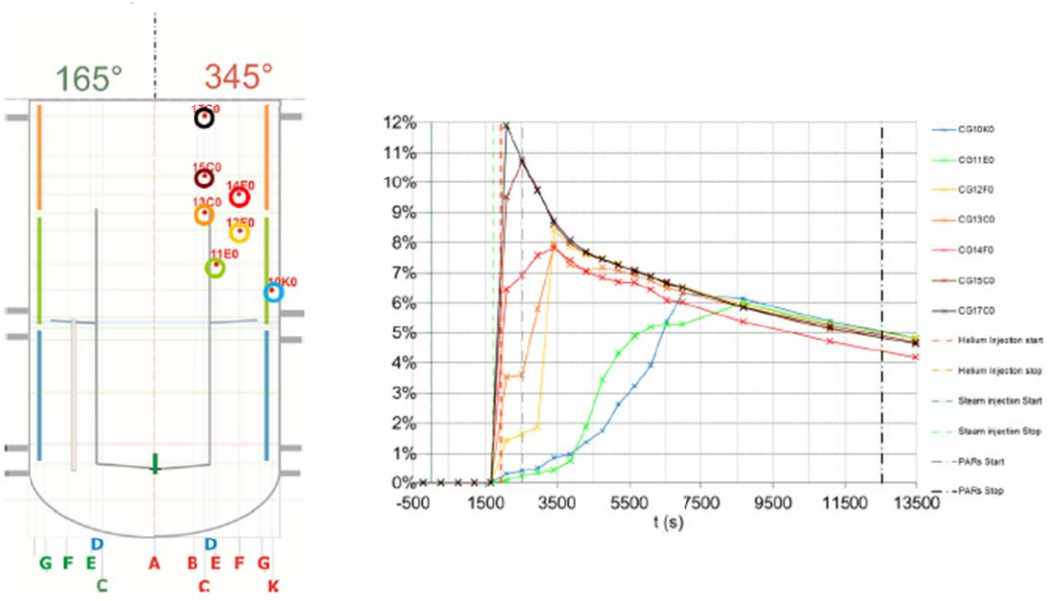

Figure 14: Color map according MERCO3-1 test (left) and short term helium concentration evolution (right) [26].

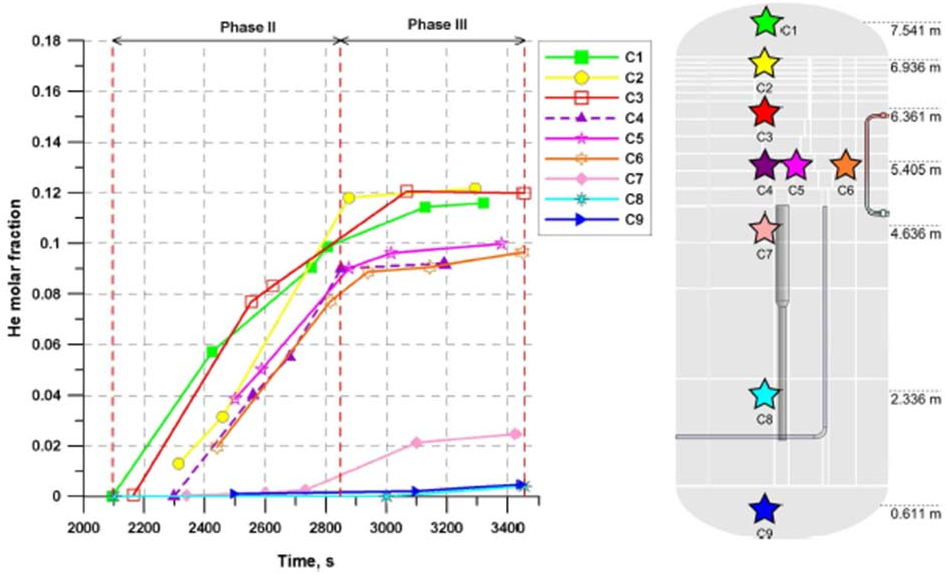

Figure 15: Helium molar fraction during Phase 2 and 3 in SPOT test [28].

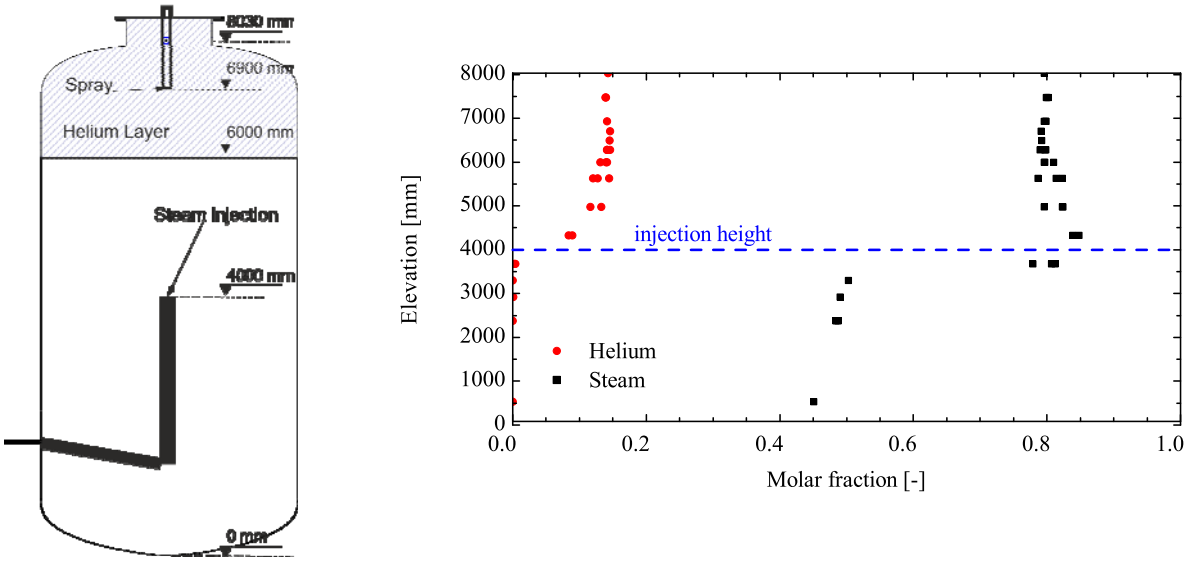

Figure 16: PANDA steam/helium molar fraction at the end of Phase 3 for PE1 test over the Vessel 1 height [29].

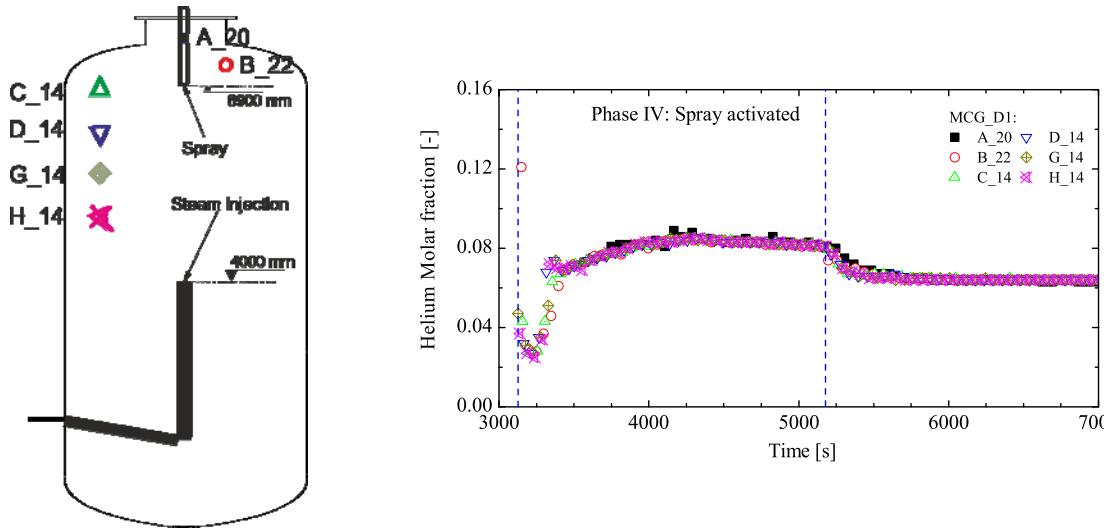

Figure 17: Helium molar fraction in PE1 test [29].

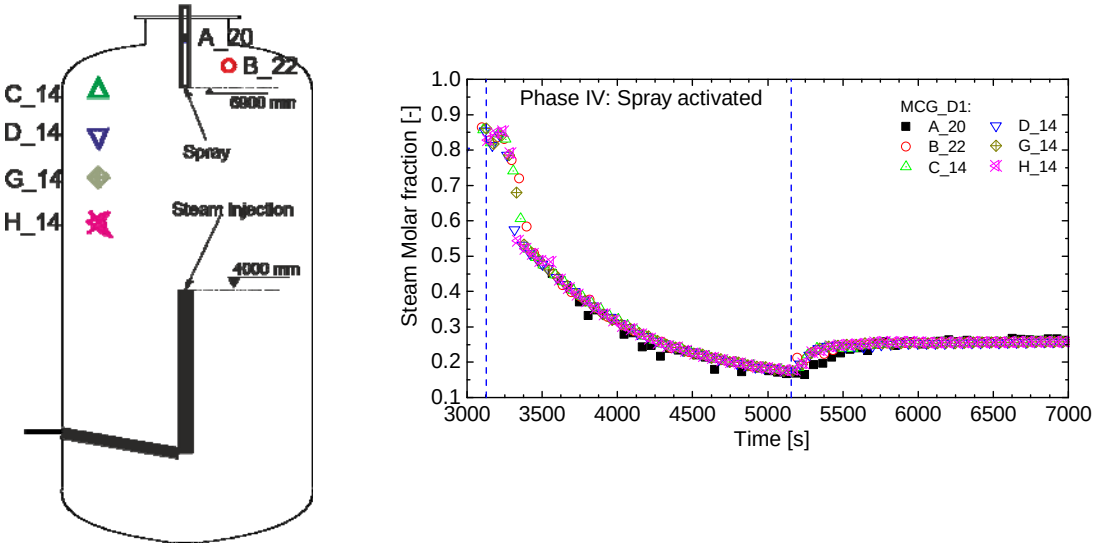

Figure 18: Steam molar fraction in PE1 test [29].

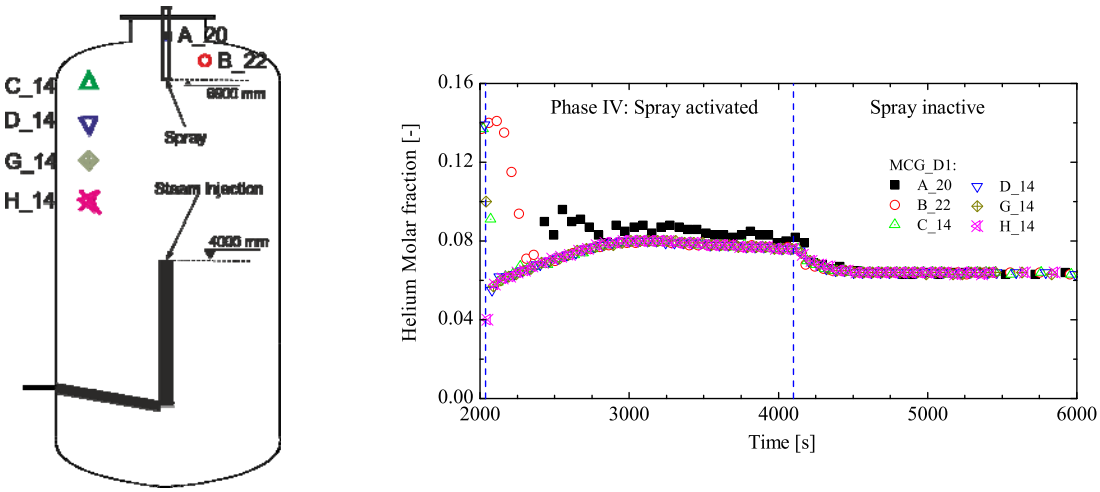

Figure 19: Helium molar fraction in PE2 test [30].

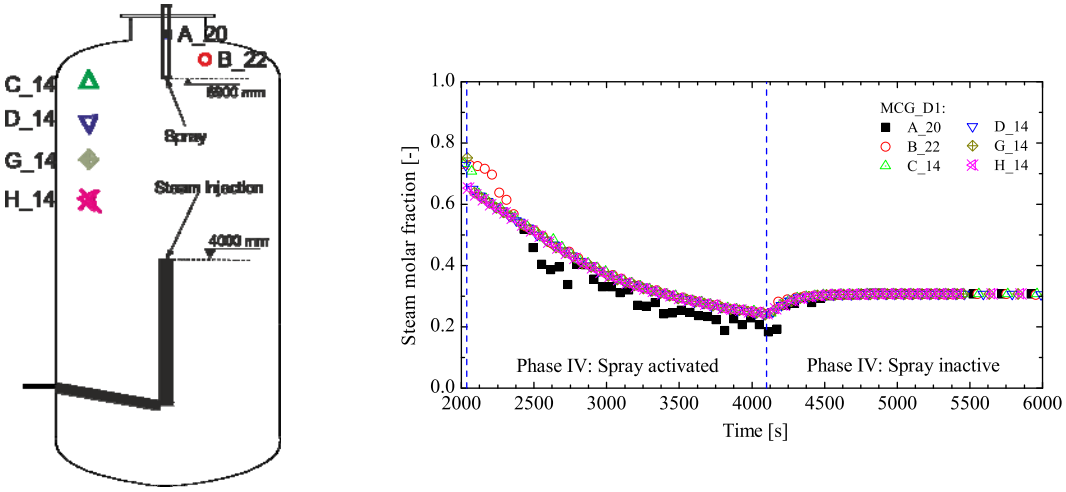

Figure 20: Steam molar fraction in PE2 test [30].

In the tests performed with activation of a cooler, the containment pressure decreased more slowly than in the spray tests. In the PE3 test the pressure decreased from 2.5 bar to 1.47 bar in 7710 s (Figure 12 and Figure 21) and in PE5 from 2.5 bar to 1.35 bar in 7262 s (Figure 22). In MERCO_2, the pressure decreased from 2.56 bar to 2.2 bar in 2500 s (Figure 23). In the S1 test the pressure decreased from 2.5 bar to 1.2 bar in 9380 s (Figure 24) and in the S2 test from 2.5 bar to 1.2 bar in 9304 s (Figure 25).

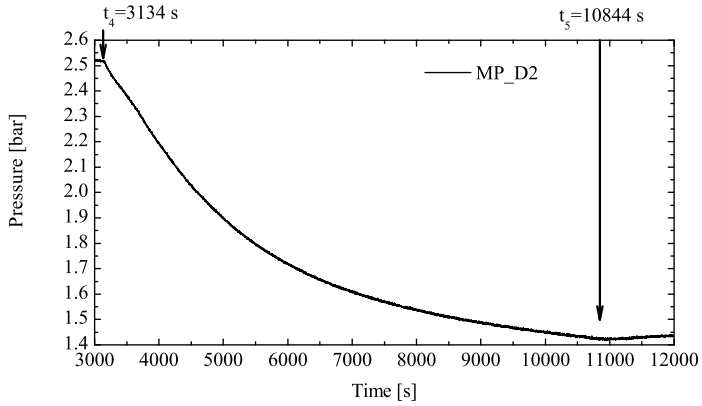

a) Pressure evolution in PANDA vessel during Phase 4 of test PE3.

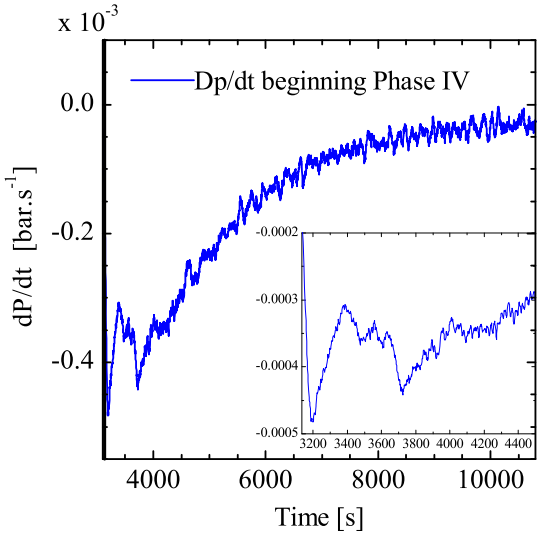

b) dP/dt for Phase 4 of test PE3.

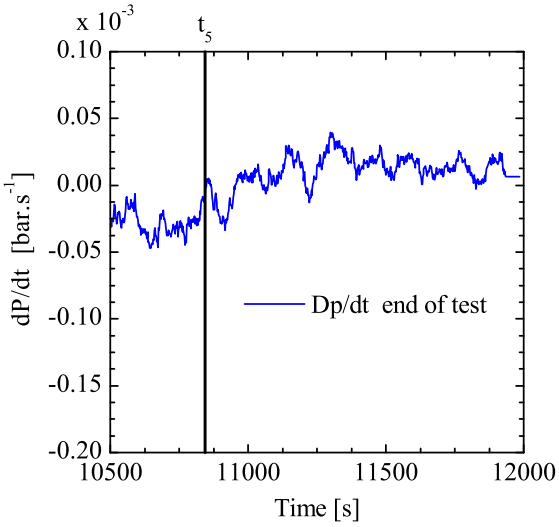

c) dP/dt after Phase 4 of PE3.

Figure 21: Pressure evolution in PANDA vessel during Phase 4 of test PE3 [31].

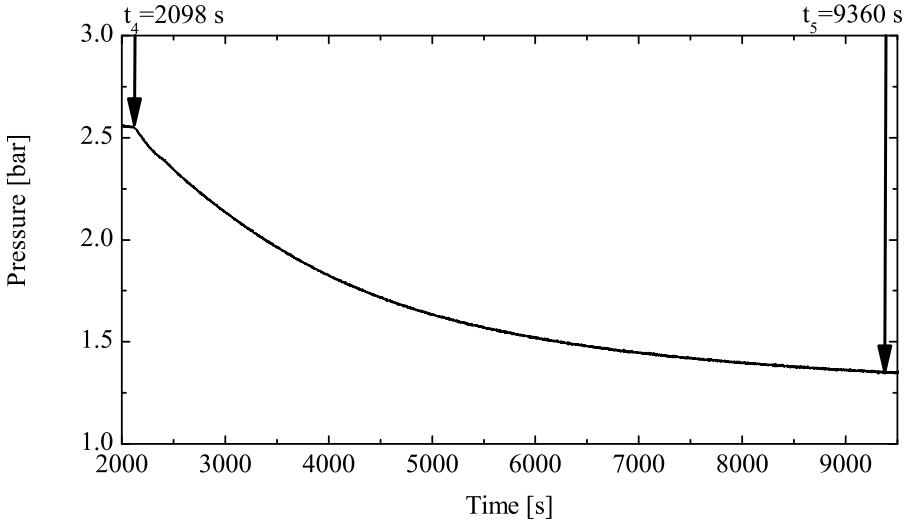

Figure 22: Pressure evolution during PE5 test [33].

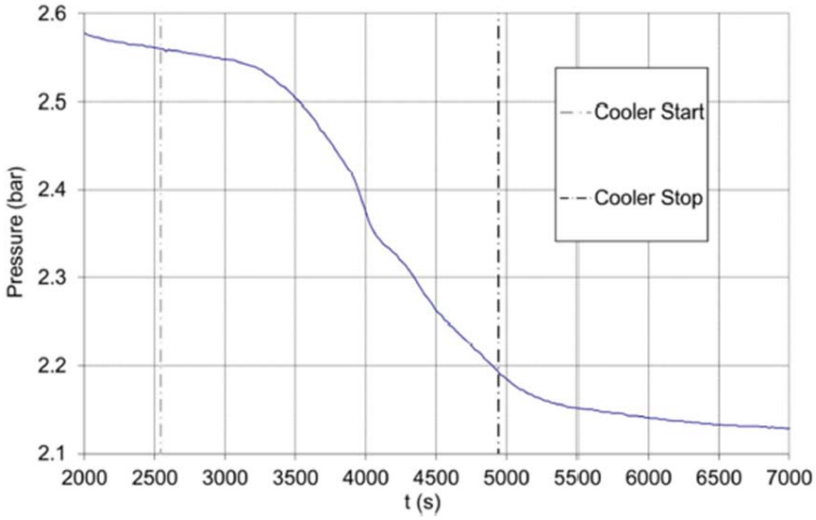

Figure 23: Pressure evolution during MERCO-2 test (Phase 4) [25].

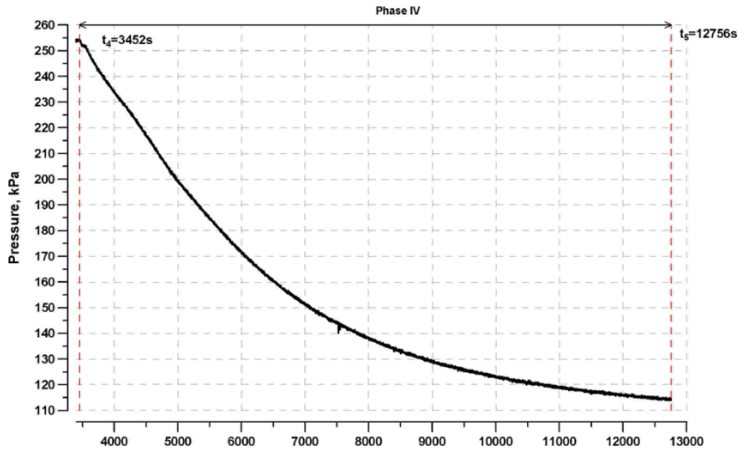

Figure 24: Pressure evolution during S1 test (Phase 4) [28].

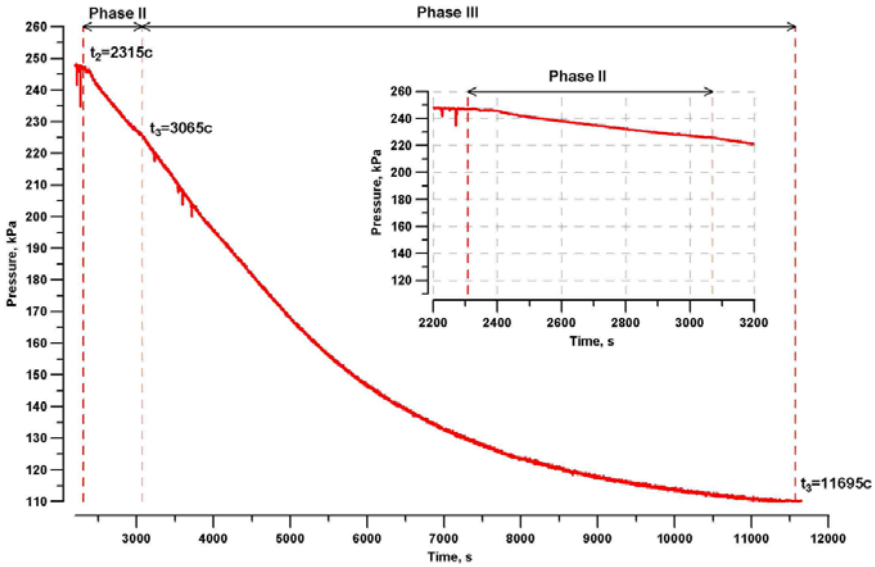

Figure 25: Pressure evolution during S2 test (Phase 4) [28].

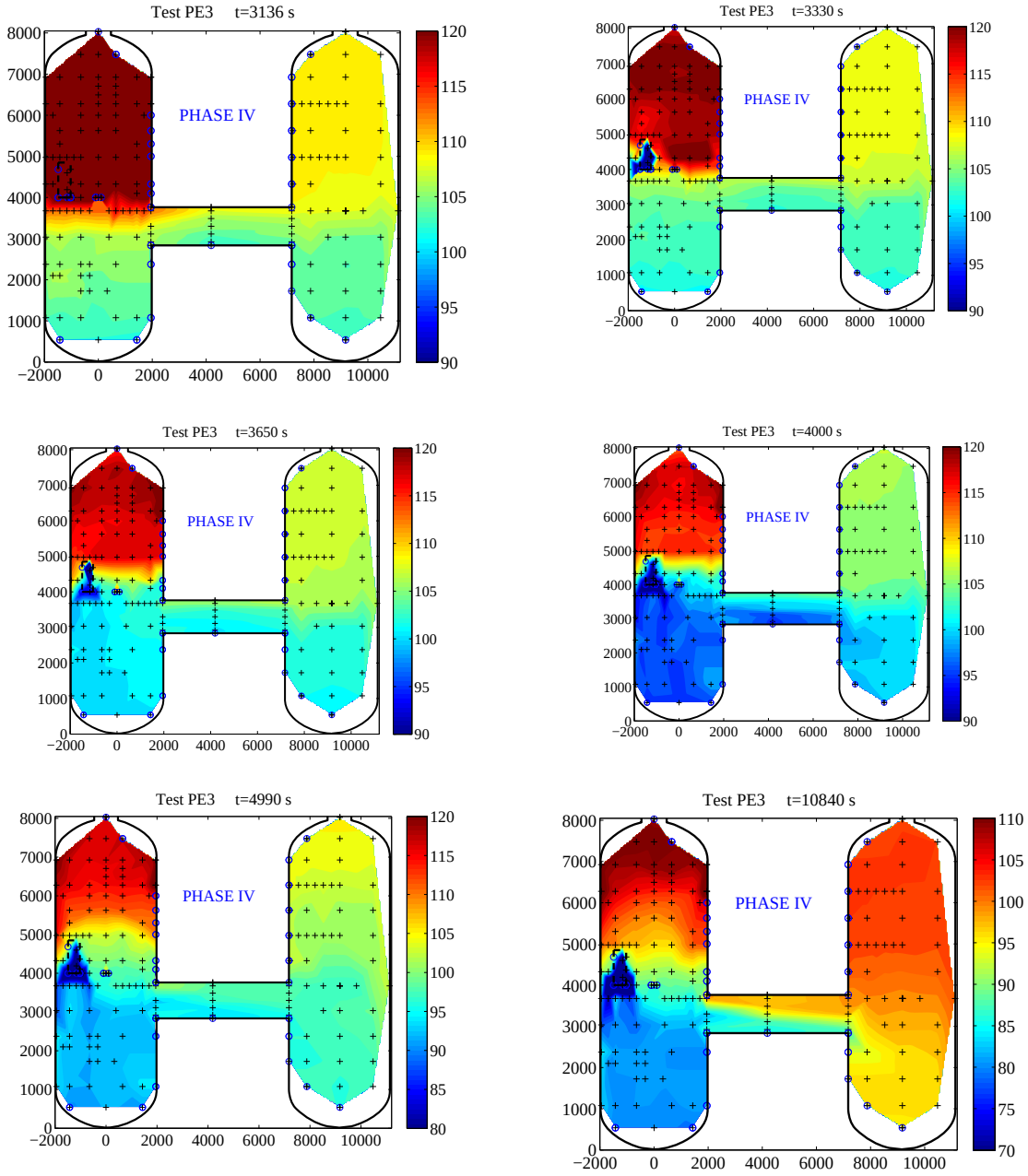

Figure 26: Selected temperature contour maps measured in PANDA vessels during selected times in PE3 test (Phase 4).
The cooler can be identified as the coldest region in Vessel 1 [31].

The evolution of gas species, in particular the cooler's capability to destabilize a stratified hydrogen atmosphere, is related to the release conditions (radial and vertical release locations) for the given scenarios, the cooler design (exposed cooler tubes, or tubes inside a case with closed faces), the cooler position within the containment and with respect to the release location.

The cooler used in PE3 and PE5 tests was installed in the middle region of the PANDA containment, and the cooler design included cooling pipes inside a frame with open sides (leaving a possibility for the helium/steam/air mixture to leave the cooler flowing through the cooler pipes). The convection induced by the cooler was confined within 1 m above the cooler and therefore the helium rich-layer was only partially eroded (see e.g. temperature maps in Figure 26 and steam/helium molar fraction in Figures 27-30).

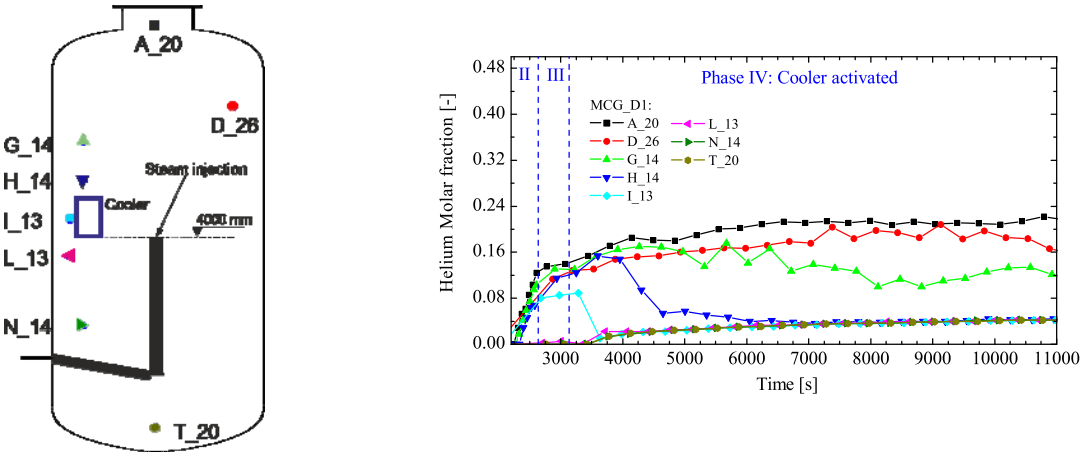

Figure 27: Helium molar fraction during PE3 test [31].

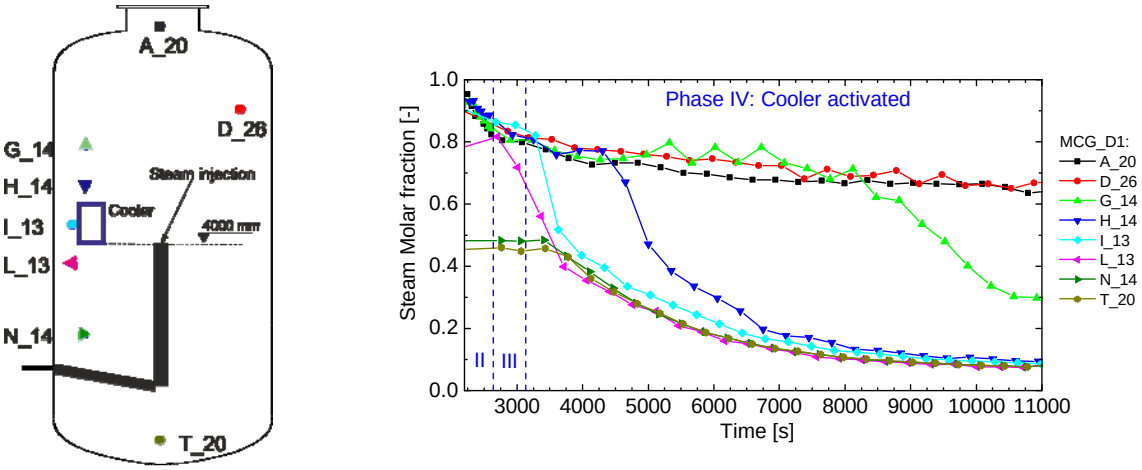

Figure 28: Steam molar fraction during PE3 test [31].

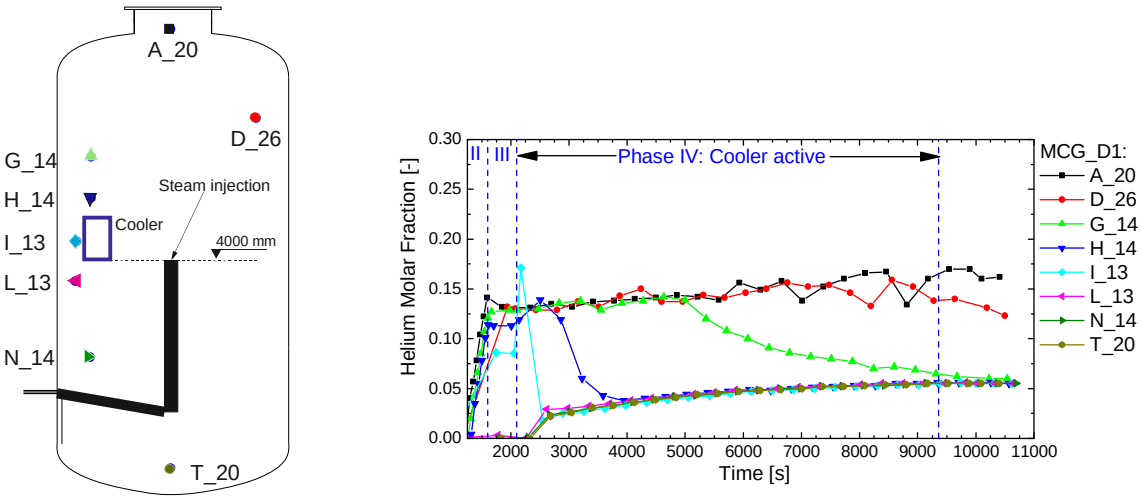

Figure 29: Helium molar fraction during PE5 test [33].

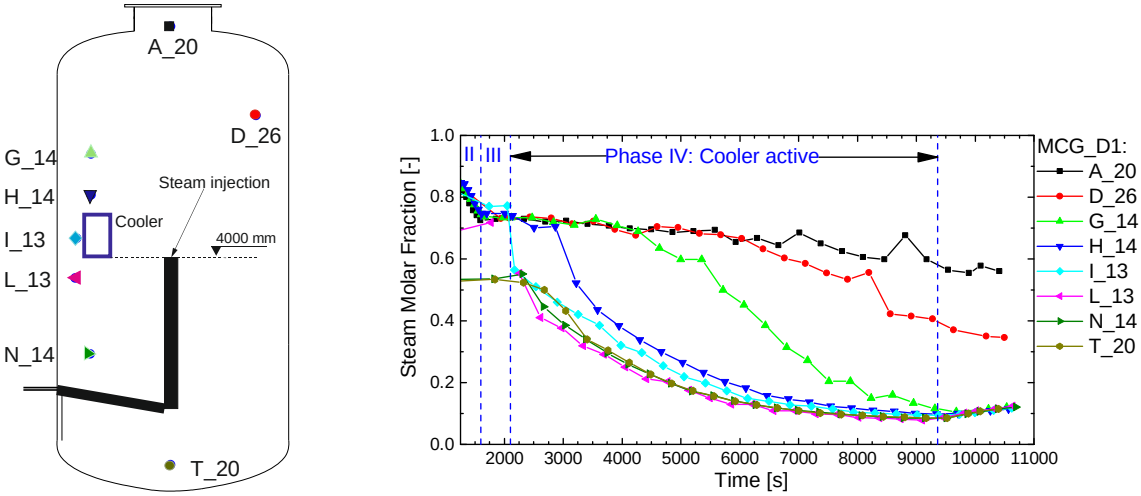

Figure 30: Steam molar fraction during PE5 test [33].

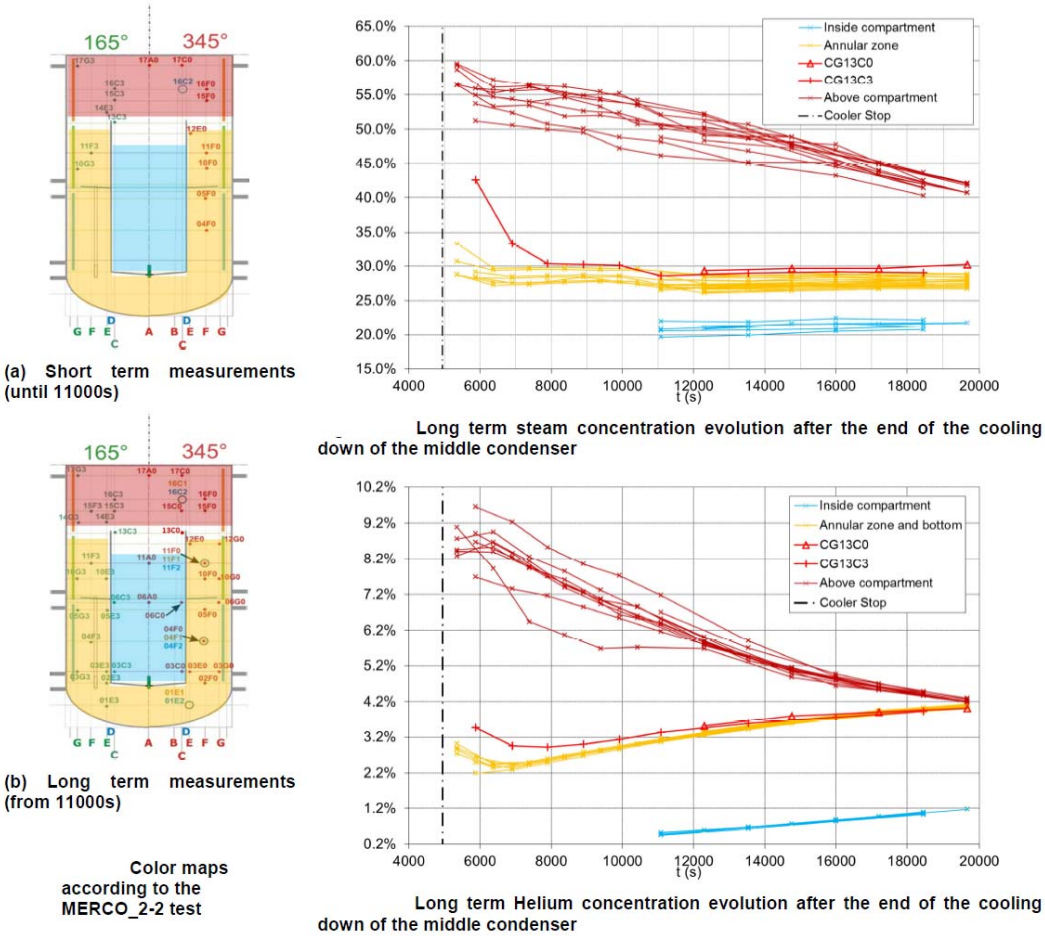

Figure 31: Steam/helium concentration during MERCO-2 test [25].

In the MERCO-2 test, with activation of the condenser installed in the medium elevation of the MISTRA containment, a stratified atmosphere consisting of two main zones persisted until the end of the test. A helium-rich layer remained in the free volume above the internal MISTRA compartment. Below the helium-rich layer, in the annular space between the condenser and the compartment and above the annular ring, remained a stable air-rich mixture (Figure 31).

In the S1 and S2 tests, the convection induced by the cooler activation also led to a partial erosion of the helium-rich layer located in the upper region of the facility (see helium/steam concentration evolution in Figures 32-35). Moreover the activation of a cooler in the S2 test during the helium-release phase did not produce qualitative differences in the helium-rich layer break-up.

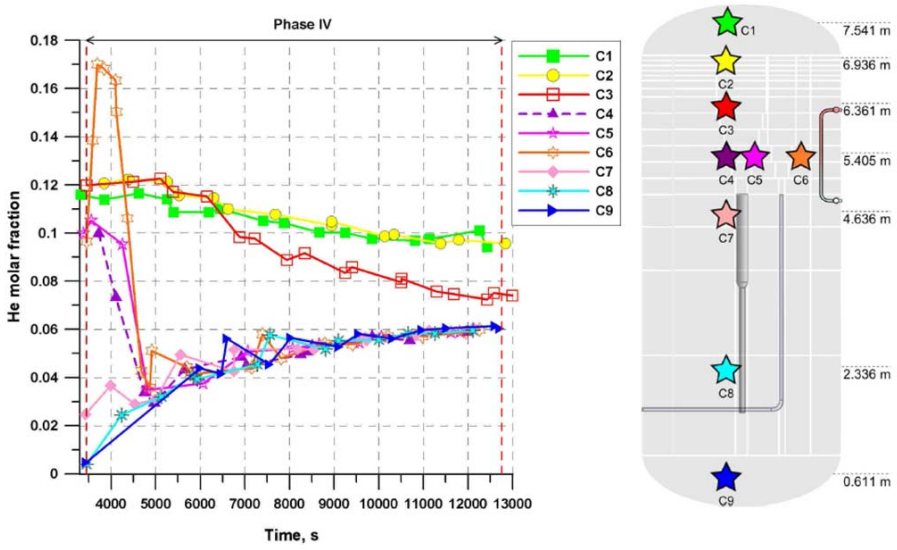

Figure 32: Helium concentration during S1 test [28].

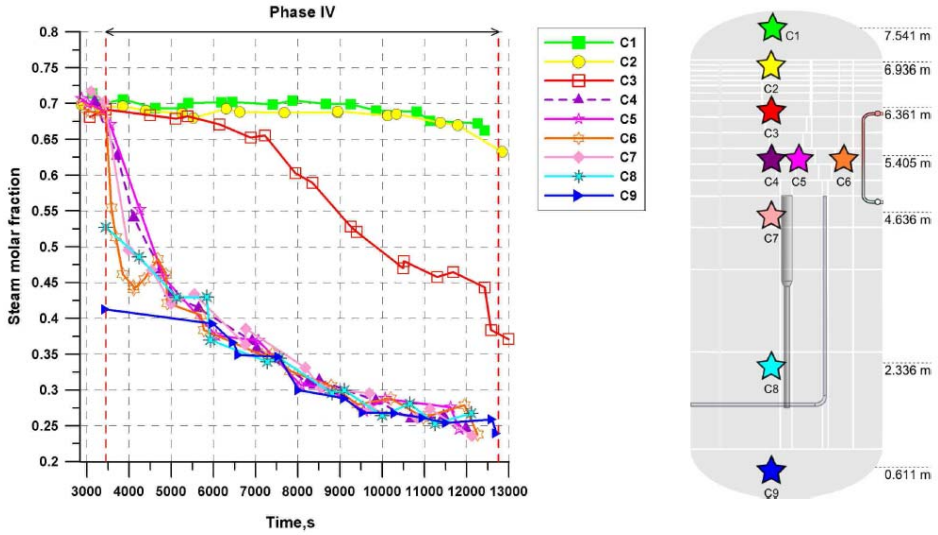

Figure 33: Steam concentration during S1 test [28].

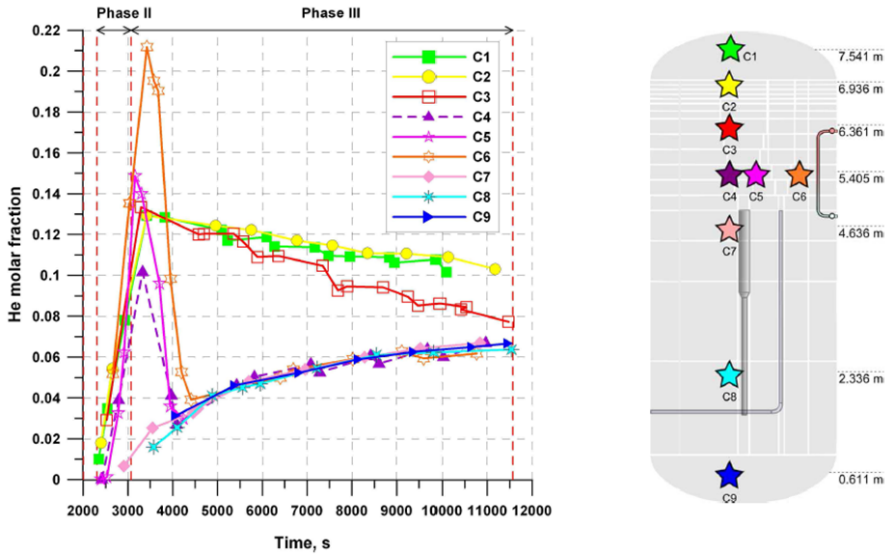

Figure 34: Helium molar fraction during S2 test [28].

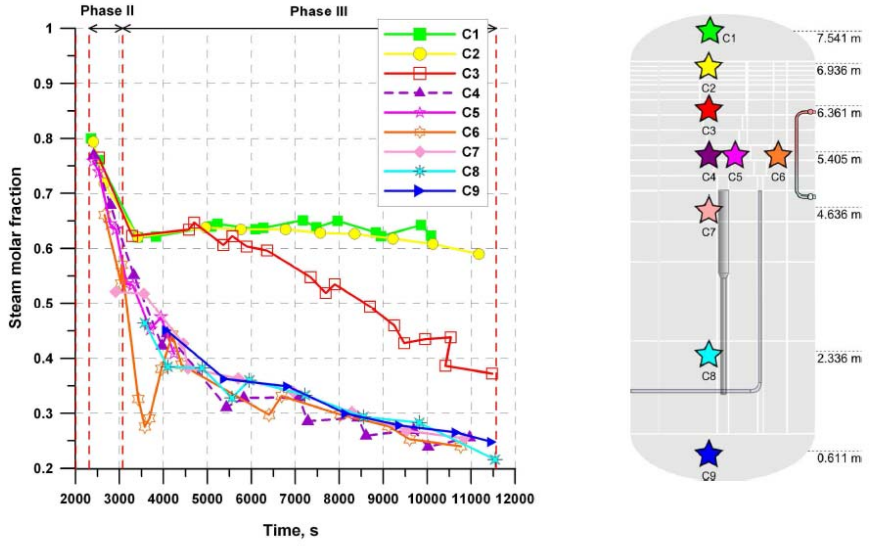

Figure 35: Steam molar fraction during S2 test [28].

In the tests performed with activation of a heater, the energy released to the gas had a minor effect on the gas pressure evolution. In the PE4, MERCO_3 and MERCO_4 tests the heat loss from the facility walls prevailed over the heat source by the heater/s and the pressure slightly decreased during the heater activation. The convection induced by the heater in PE4 led to complete homogenization of the gas mixture located above the heat source inlet elevation (see helium/steam concentration evolution in Figures 36 and 37).

A gas mixture with a lower helium content slightly diffused downward and flowed through the top of the IP towards Vessel 2. Nonetheless the heater effect on gas mixing in the region below the heater was rather limited.

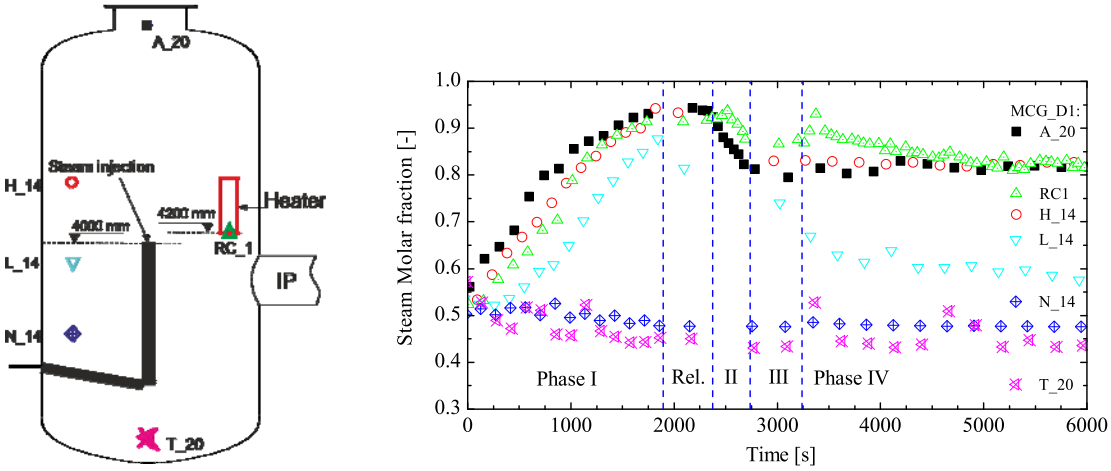

Figure 36: Steam concentration during PE4 test [32].

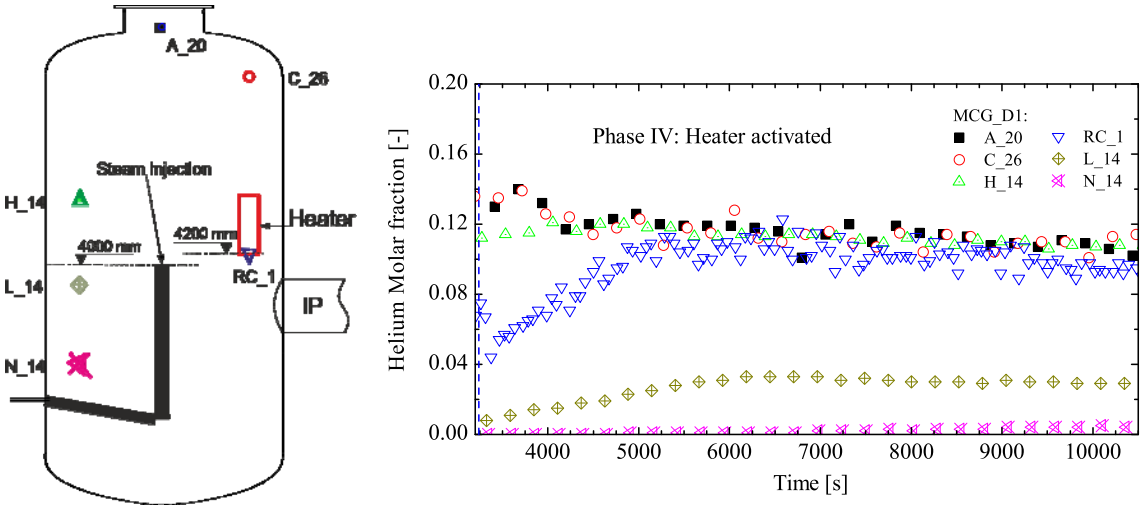

Figure 37: Helium concentration during PE4 test [32].

In MERCO-3 and MERCO-4, with the heater located in the upper compartment region, the helium homogenization extended to the elevation of the ring plate, and the facility compartments allowed the creation of flow patterns ing to the transport of helium below the heater elevation (see steam/helium concentration evolution in Figure 38 (MERCO-3) and Figure 39 (MERCO-4)).

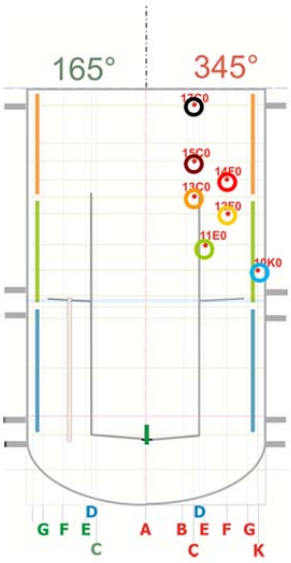

Color map according to the MERCO_3-1 test - Short term concentration evolution

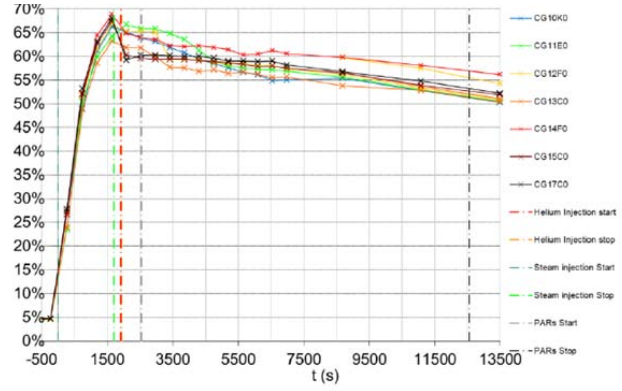

Short term steam concentration evolution – MERCO_3-1

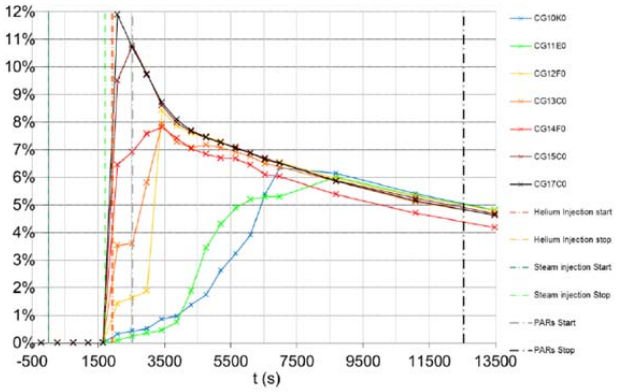

Short term Helium concentration evolution – MERCO_3-1

Figure 38: Steam/helium concentration during MERCO_3-1 test [26].

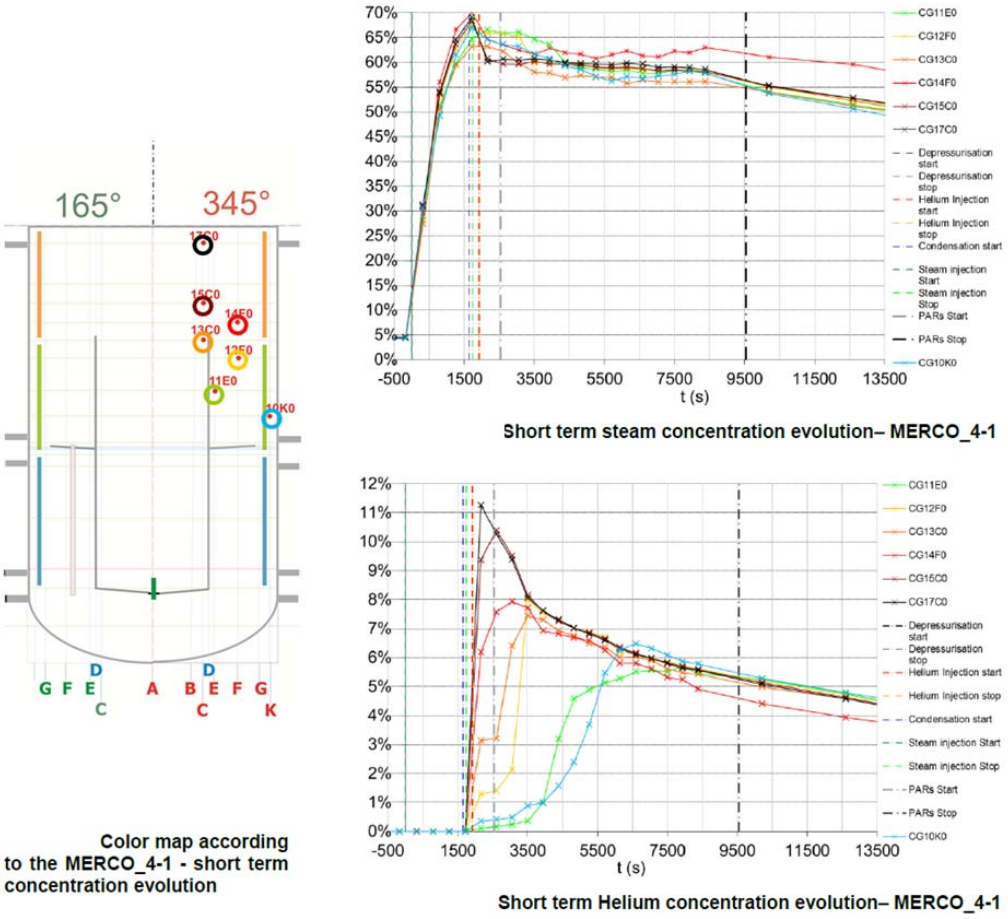

Figure 39: Steam/helium concentration during MERCO_4-1 test [26].

The data have provided an excellent database for the assessment of the computational tools, and an impressive number of simulations have been performed within the ERCOSAM project. These simulations are listed in [58], which also includes the contributions to the HYMIX numerical exercise. For practical reasons, also the codes GOTHIC and GASFLOW will be referred to as “CFD” codes.

Due to the large number of contributions, only examples of the results obtained within the project will be discussed below. The discussion will be focused on the results of simulations with CFD codes, whereas the performance of LP codes is discussed only for the cases when their predictions are notably different from those obtained with CFD codes. A more complete survey is included in [58] and in the reports prepared by each Organization. The focus, here, will be on the results for the two large-scale facilities PANDA and MISTRA, because in TOSQAN some specific effects prevailed in the spray tests, and extensive analysis of the results of the SPOT tests is included in the corresponding SAMARA report [57].

The analysis of the TOSQAN, MISTRA, SPOT and PANDA tests allowed insight on the actual code capabilities and on the modeling needs to simulate the tests. The two step approach (pre-test

simulations: [34-43] and post-test simulations: [44-57]), led in general to improved simulation results in the post test analysis, with respect to the pre-test analysis. Indeed, the major discrepancies of the code simulations with the test results, identified with the pre-test analysis, were eliminated by using a more complete and accurate set of test initial and boundary conditions (actual test conditions instead of nominal values). Therefore the pre-test analyses, which nevertheless showed the capability of the codes to reproduce the main trends with respect to the main phenomena, cannot be considered as fully representative of the code capabilities to perform blind simulations. They have been very useful, however, because they contributed to a closer look at all the available experimental data and revealed some technical issues, which could be properly addressed in the post-test analyses.

In general, the post-test analyses were rated “reasonably” good, which, in absence of some criterion to quantify the accuracy, is appropriate for most contributions (excluding those, as discussed below, which report “work in progress”). In the Synthesis Report [58], a few parameters have been selected to compare the performance of the codes, but these success indices could not be used for a real rating of the simulations. Actually, during the project the question was raised on the issue of how to quantify the success of the various simulations, but no criterion could be identified that could serve for all codes and types of tests. Indeed, the development of some objective quality indicators is a challenge (and still an unresolved issue) for any future project aiming at the assessment of codes used for containment safety analysis.

With respect to the Phases 1, 2 and 3 of the experiments with wall condensation, the codes in general predicted the pressurization rate well in the post-test analysis. Figure 40 provides two examples of results for tests with condensation in PANDA, which show a nearly perfect agreement. Although other simulations showed some deviations (but smaller than 5 kPa at the end of Phase 3), in general the pressurization phase was predicted very well. Since the transient was controlled by wall condensation (and, as shown later by the initial conditions, which strongly affect the condensation rate), it can be concluded that all various condensation models used in the different codes performed very well.

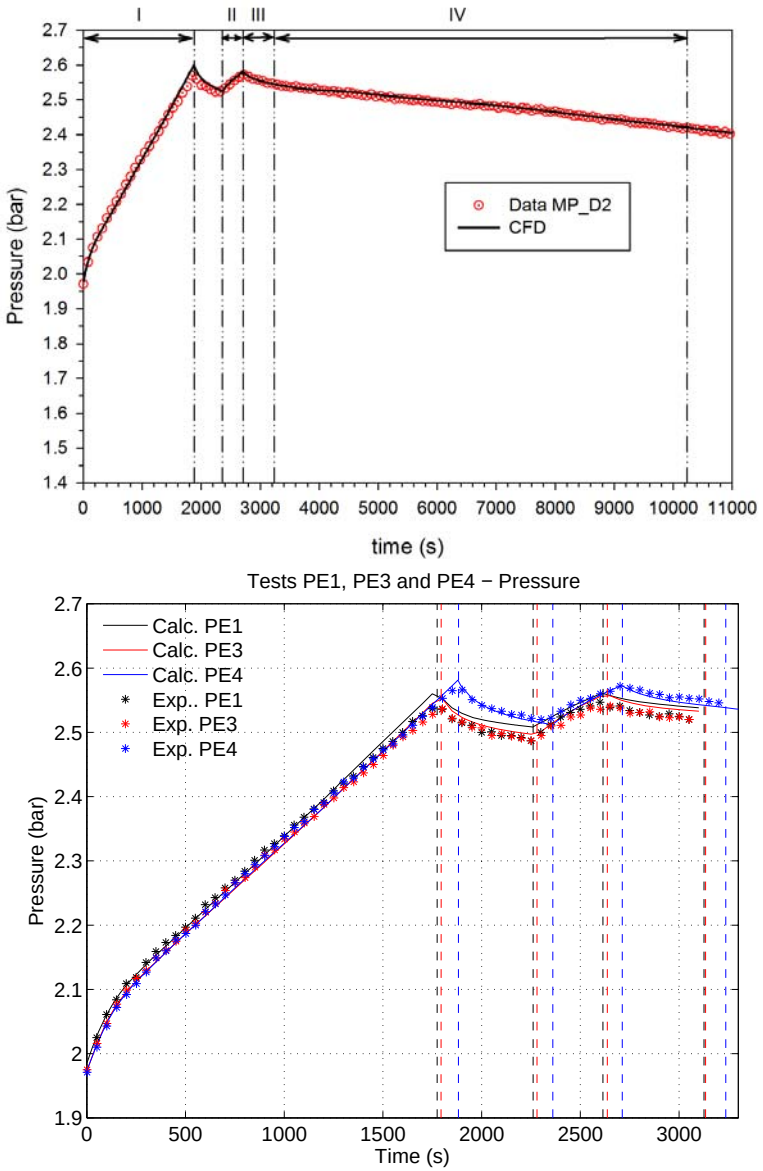

Figure 40: Pressurization in PE4 test calculated using (from top to bottom), FLUENT [46] and in PE1, PE3 and PE4 tests using GOTHIC [47].

The substantial improvement with respect to the pre-test analyses (Figure 41) was mainly due to the correct calculation of the condensation rate (including spurious contributions due to heat losses) and the use of the correct steam/helium sources. In the post-test analyses the detailed initial distributions of gas concentration and wall temperature, the actual heat losses and nominal values for the steam and helium injection rate could be used, and the correct setting of initial and boundary conditions was crucial for the success of the simulations. In particular, the wall temperature and the initial gas concentrations had a major effect on the pressurization rate. A difference of few degrees (~2-3^{o}C) in

wall temperature and a few percent in molar fractions had a major effect on the containment pressurization rate.

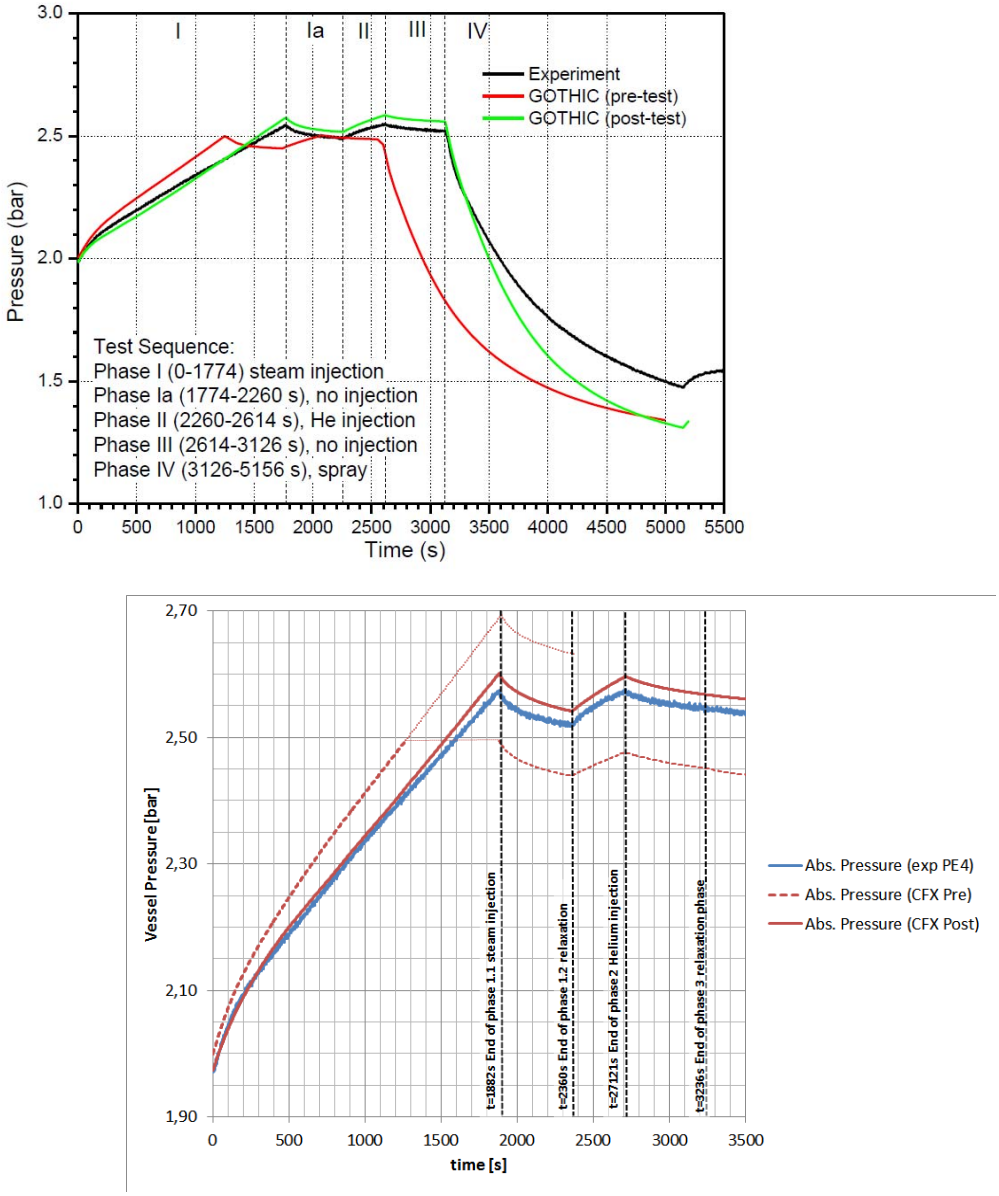

Figure 41: Effect of initial and boundary conditions on the improvement of results in post-test analysis for tests in PANDA. From top to bottom: calculations for PE1 test with GOTHIC [44] and PE4 test with CFX [54].

Figure 42 shows representative results for tests in MISTRA, where also the effects on the results of more accurate modelling of spurious condensation and parasitic heat transfer rates from the condensers are displayed. It can be noticed that the results of the code are consistent with each other, as they display the same discrepancies with the experimental curve, which suggests that further

refinements in the representation of the facility-specific heat transfer effects could led to even better results.

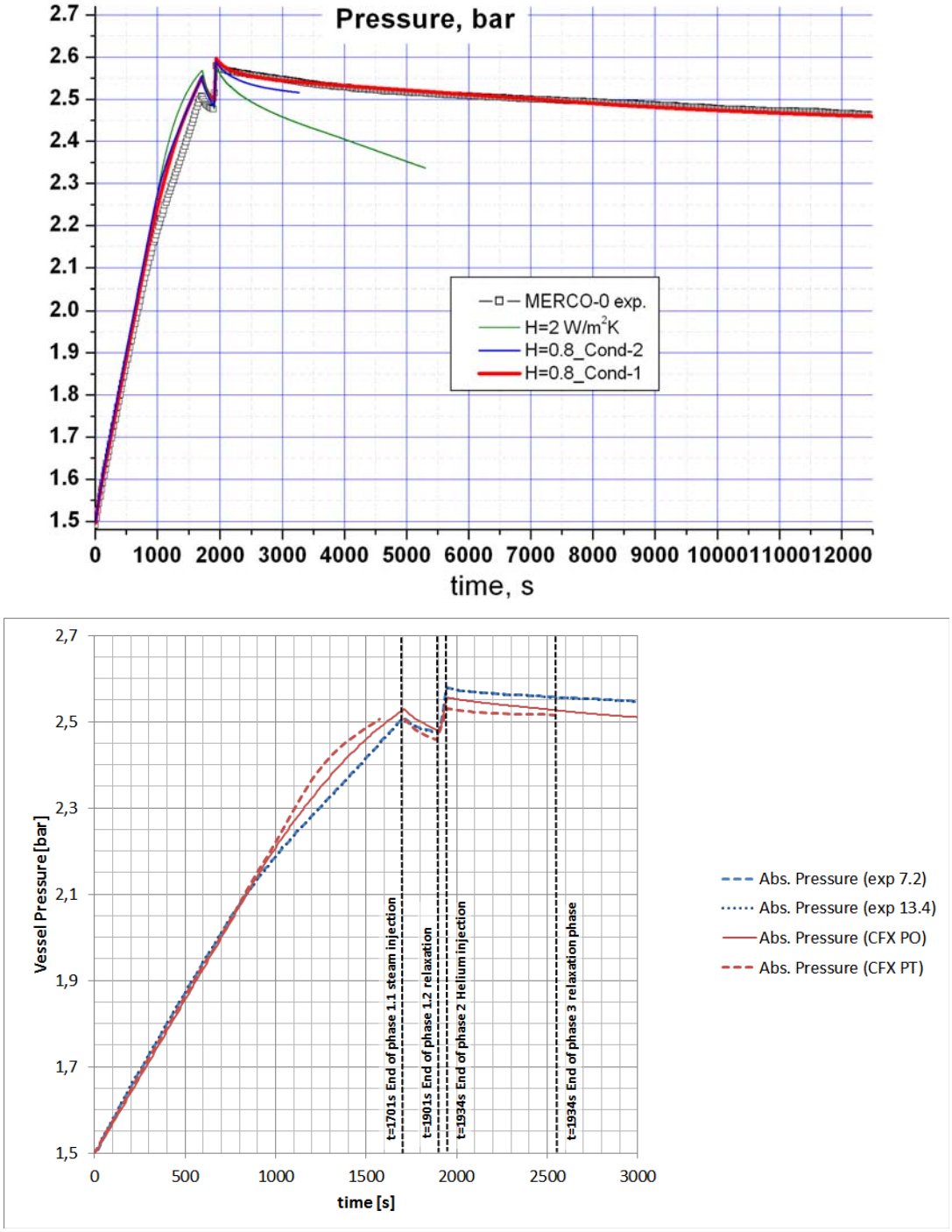

Figure 42: Pressurization in MERCO-0 test calculated using (from top to bottom): FLUENT [46] and CFX [54].

The pressure time history in TOSQAN T115 tests could also be predicted very well, as shown by the simulations with FLUENT and GOTHIC in Figure 43. In this case, the condensation to be predicted was that resulting from the operation of the temperature-controlled condenser (cold section of the double-wall vessel). The results of pre-test analyses were also very accurate, and therefore are not shown.

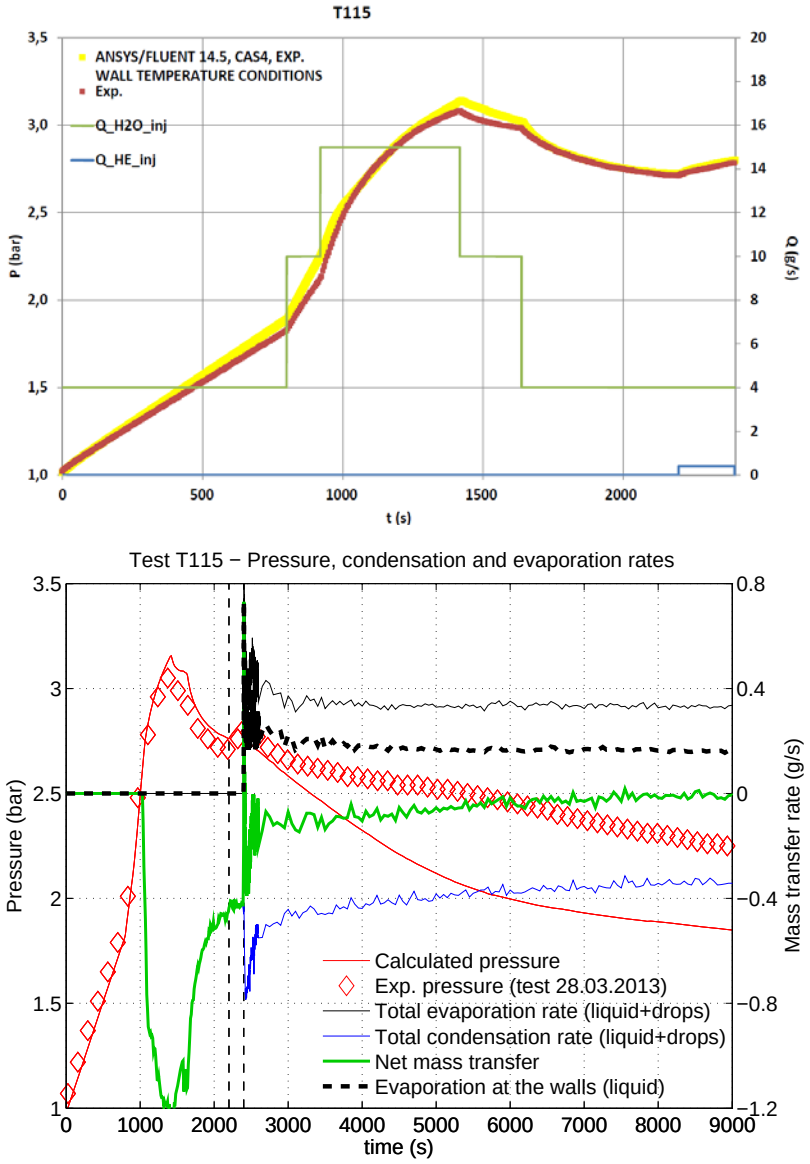

Figure 43: Pressurization in T115 test calculated using (from top to bottom): FLUENT [49] and GOTHIC (complete transient, [47]).

Figure 44 shows the results of both pre-test and post-test calculations for Test S1 in SPOT. In this case, the code results could be directly compared. It is observed that the post-test predictions (for contributions that included both pre-test and post-test analyses) were substantially more accurate than the pre-test results, mainly due to the consideration of the actual mass and distribution of the

metal mass and the actual initial and boundary conditions (which were somewhat different from those prescribed in the test protocols).

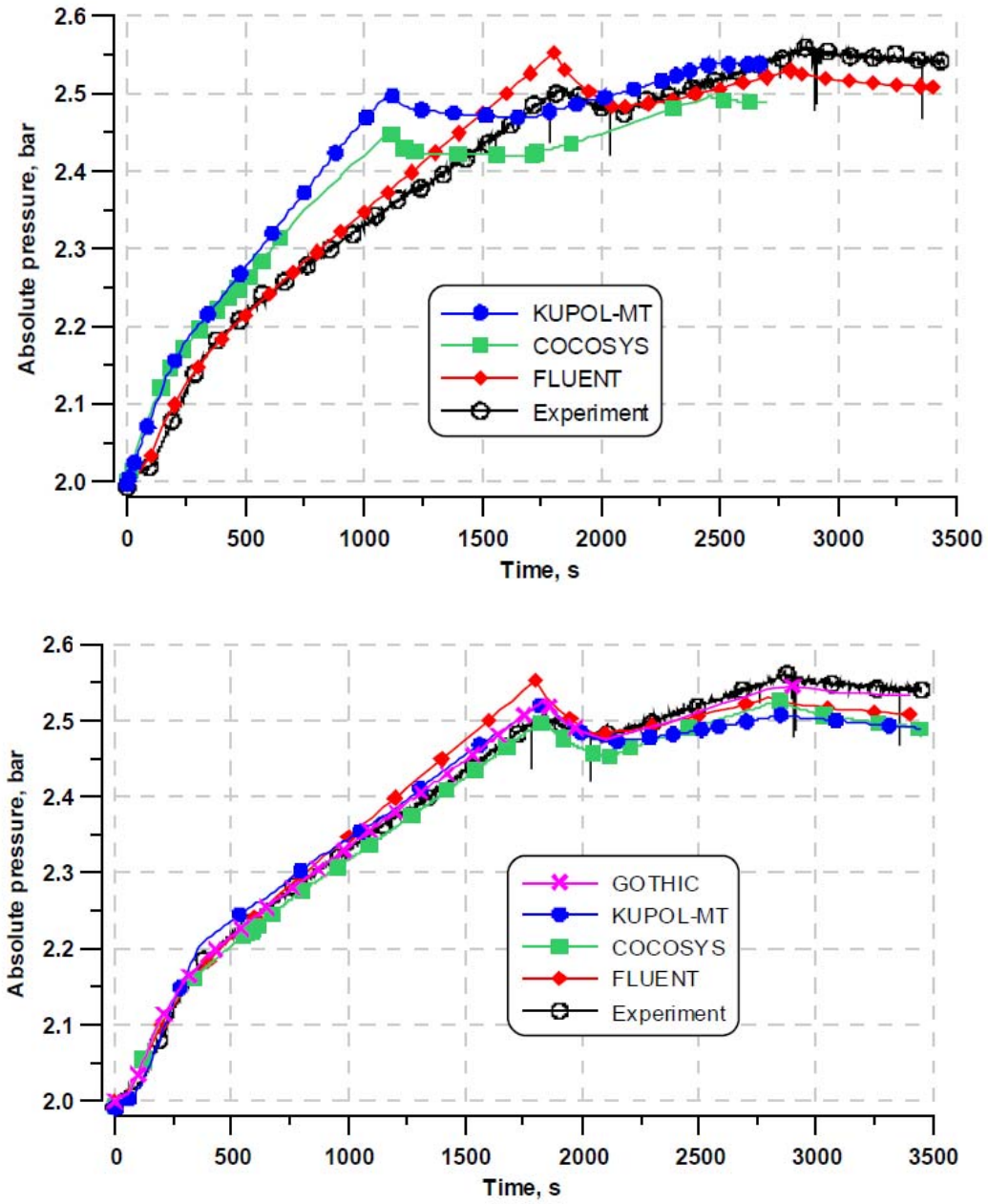

Figure 44: Comparison of pre-test (top) and post-test (bottom) results obtained with various codes for S1 test [57] for all tests with condensation, various sensitivity studies, such as improving mesh resolution near the wall, modifications in the modelling of wall heat transfer, refined modeling of wall condensation (including spurious effects) also contributed to improve the simulation results.

For tests without wall condensation, wall heat transfer played a dominant role, and the effect of radiative heat transfer, although debated, in some simulations has been shown to be an important

one. This effect could be especially large in regions where the fluid is nearly stagnant, such as the region (below the elevation of the exit of the injection pipe) across the density interface during steam/helium injection. Indeed, most simulations in this region predicted too high of temperatures due to compression heating effects, not compensated by adequate wall transfer. Although these phenomena played a role in gas and wall temperature distribution (which were not reproduced accurately), the pressure was generally well predicted, and the quality of the results of the post-test analyses was only marginally higher than that of the pre-test analyses. The results of the post-test simulations for tests PE2 and PE5 in PANDA and T116 in TOSQAN are shown in Figures 45 and 46, respectively. For tests in PANDA (Figure 45), it is observed that some deviations remained, mostly attributed to inaccurate representation of the wall heat transfer.

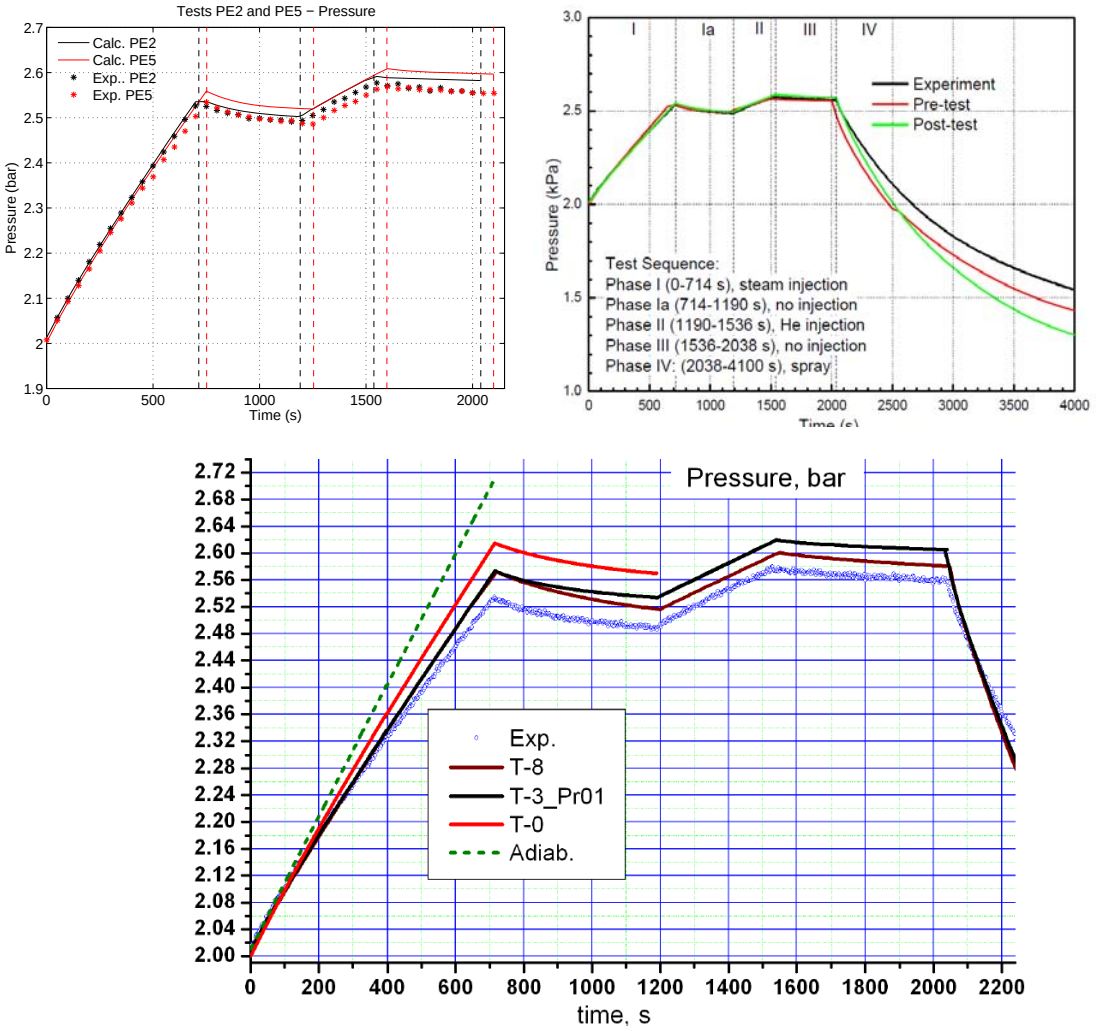

Figure 45: Results of post-test analyses of PE2 test in PANDA using (from top to bottom): GOTHIC ([47], left, and [44], right) and FLUENT [53].

In the case of Test T116 test (Figure 46), all predictions were very successful in both pre-test and post-test analysis, although some local gas temperatures (especially below the injection pipe exit) were strongly over predicted.

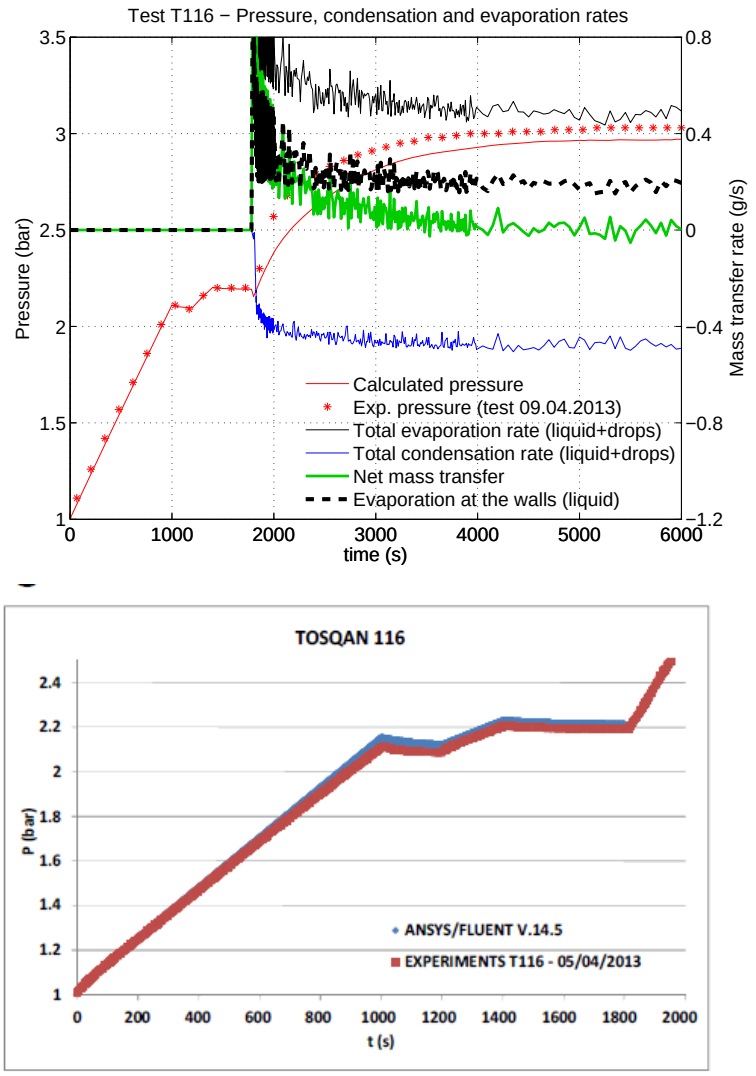

Figure 46: Results of post-test analyses of T116 test in PANDA using (from top to bottom): GOTHIC ([47]) and FLUENT [49].

The overall gas species distribution in Phases 1, 2 and 3 is predicted reasonably well over the facility height, with the exceptions of the peak helium concentration in PANDA, which could be accurately predicted only with CFX (Figure 47). The other codes over- or under- predicted the maximum value. Whereas in the case of GOTHIC the under prediction can be easily associated with the coarse mesh, difference in the predictions with CFX and FLUENT are more difficult to interpret.

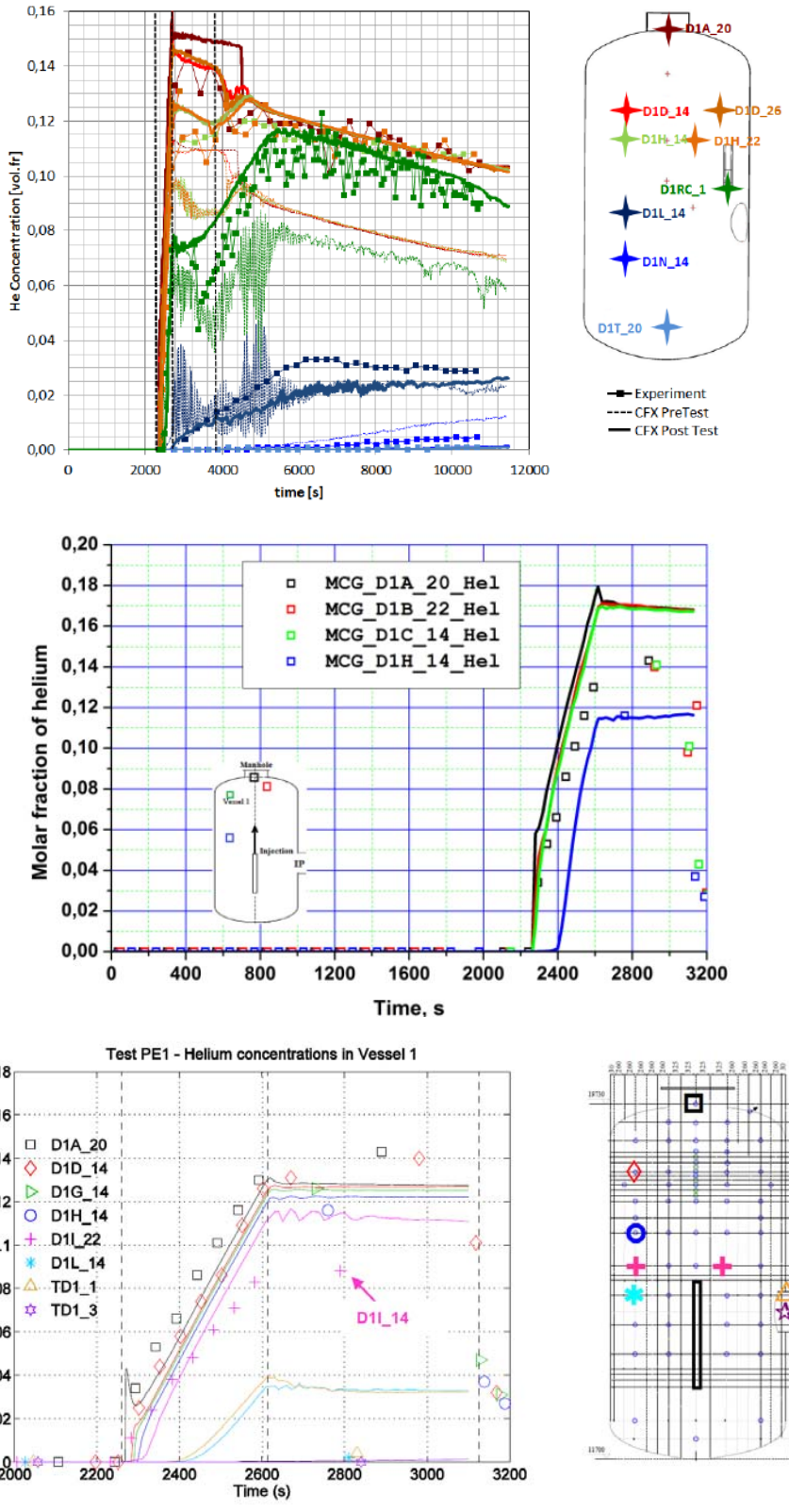

Figure 47: Helium concentrations calculated in post-test analyses for PE4 test using (from top to bottom): CFX [54], FLUENT [53] and GOTHIC [47].

Moreover, in these tests, the helium distribution in the region of the steam/helium pipe exit elevation was not accurately reproduced, with some simulations predicting too large mixing.

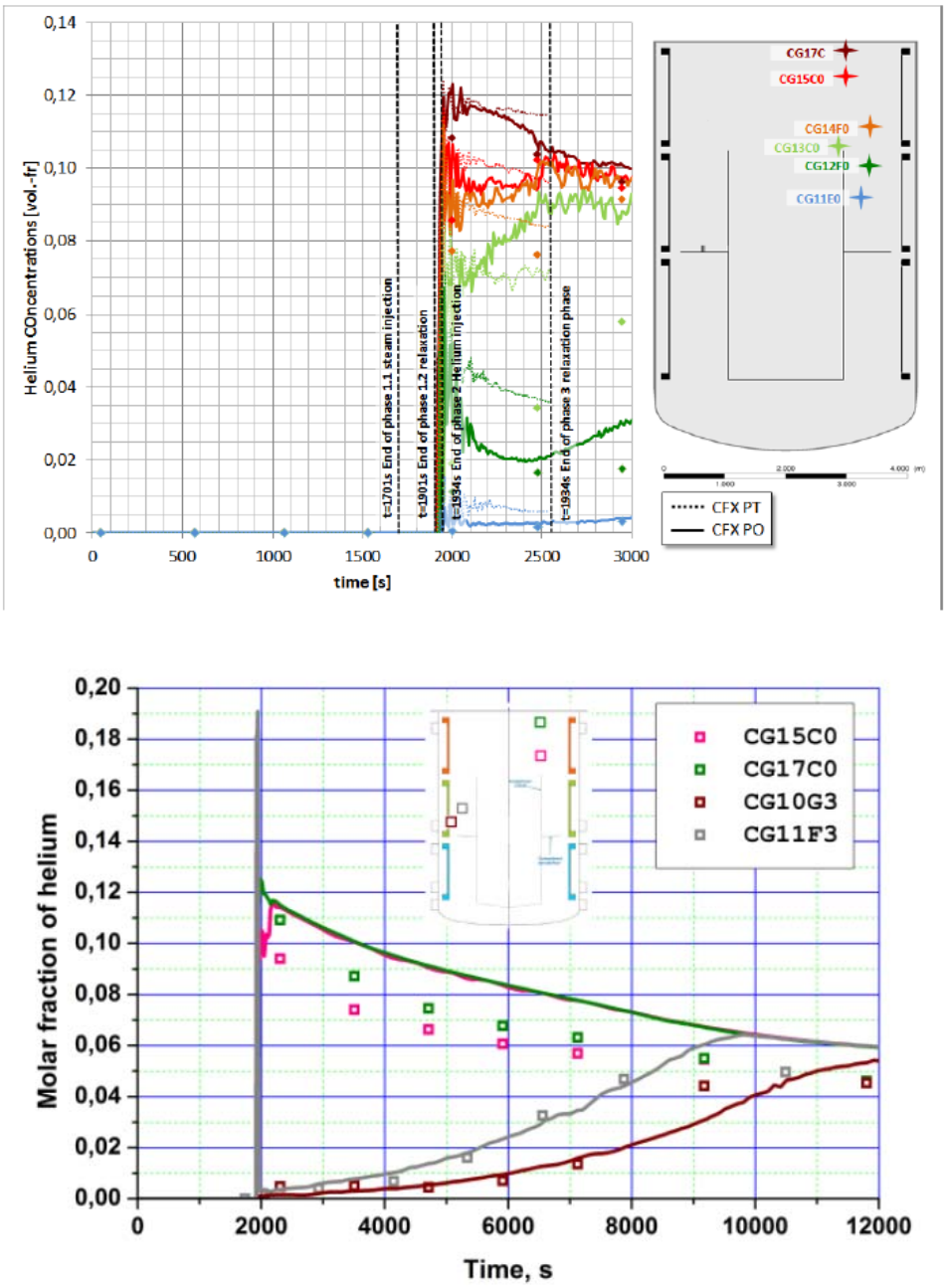

Figure 48: Helium concentrations calculated in post-test analyses for MERCO-0 test using (from top to bottom): CFX [54] and FLUENT [53].

Due to the fact that in some of the tests, (PANDA/SPOT cooler test, PANDA heater test) the release exit elevation is in the same region of the heater and cooler, the discrepancy in predicting the gas species composition in that region had a major influence in predicting Phase 4.

In the case of the MERCO-0 test, the post-test analyses (Figure 48) resulted in reasonably good predictions of the helium concentration increase at all positions. The improvements in the post-test results were mostly due to better representation of the recirculation behind the condensers.

For TOSQAN tests helium concentration measurements are difficult interpret, and therefore the performance of the codes cannot be evaluated.

Regarding the tests in SPOT, the helium vertical distribution at the end of Phase 3 in S1 test was generally well predicted, with the only main deviation observed in the prediction of the peak value (over predicted) with the FLUENT code (Figure 49). Since in S2 test the helium was injected simultaneously with the cooler operation, the performance of the codes for this test is considered in the discussion of Phase 4.

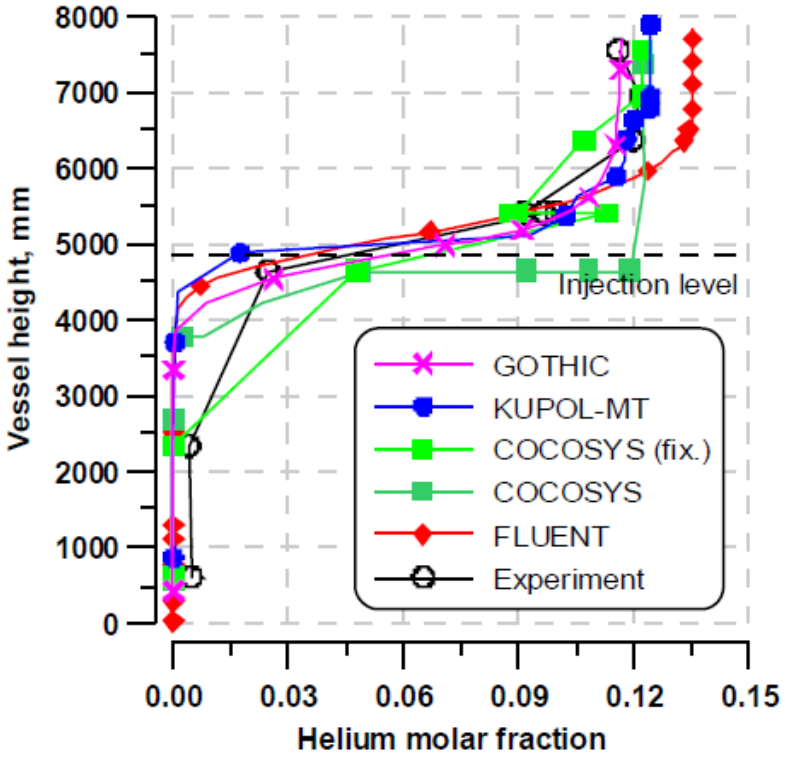

Figure 49: Comparison of the measure vertical helium concentration distribution at the end of Phase 3 in S1 and S2 tests with the predictions with various codes CFD and LP codes [57].

Phase 4, featuring the activation of the cooler, spray or heater components, was also generally well predicted by nearly all simulations.

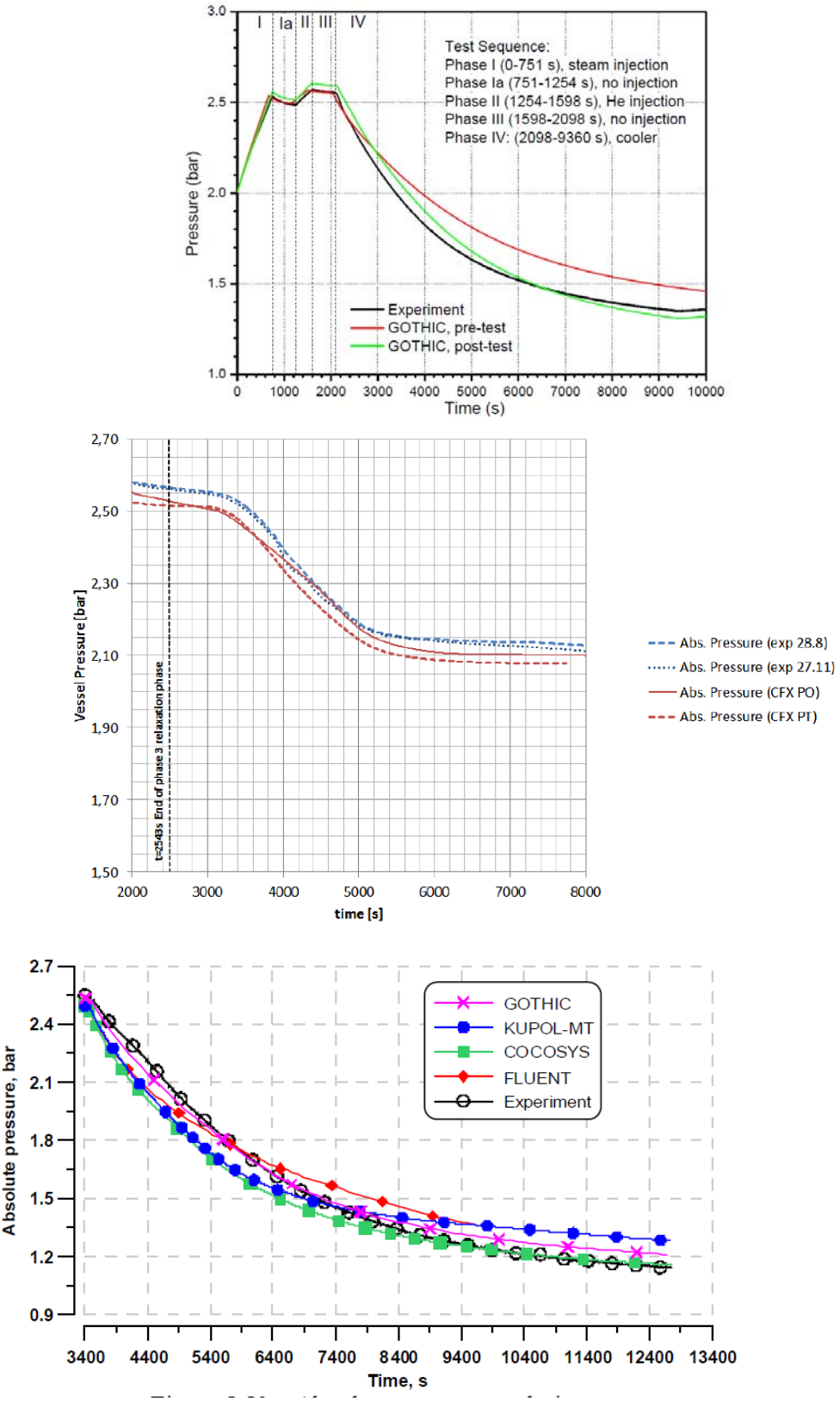

Figure 50: Pressure time histories calculated (from top to bottom) for: PE5 test with GOTHIC [47], MERCO-2 test with CFX [54] and S1 test with various codes [57].

However, due to the lack of time at the end of the project, not all post-test analyses could make use of the full experimental information and be based on model optimization, and therefore some post-test simulations, which were affected by large disagreement for some variables, should be considered as “work in progress”. Therefore, these simulations will not be considered in the further discussion of the outcome of the project.

Due to the complexity of the phenomenology and of the equipment (for tests in PANDA and SPOT), among the effects of the three types of components investigated (cooler, spray, heater), the cooler operation resulted to be the most difficult to be predicted with the computational tools. The depressurization effect was reasonably well calculated by all codes (Figure 50), and discrepancies in the pre-test analyses (as well as remaining deviations) could be attributed to inaccurate representation of certain facility specific features.

However, various discrepancies between calculated and measured results are observed in the evolution of the gas distributions for tests in PANDA and SPOT (whereas for test MERCO-0 in MISTRA the agreement was generally good).

Although, in accordance with the scoping calculations (confirmed by the experimental results) stratification was eroded very slowly in most calculations, many details of the phenomena observed in the tests could not be reproduced (Figure 51). In particular, some of the CFD simulations for some tests predicted full mixing of helium, while in the experiments a stratified atmosphere persisted until the end of the cooler operation. Moreover, the rate of the erosion of stratification was over-estimated in other tests, and this prevented the correct prediction of the evolution of the helium concentration above the cooler. In general, the cooler activation does not have an overwhelming effect on the evolution of containment phenomenology, and therefore it is reasonable to presume that the overall accident scenario depends on complex interaction between several variables and, to a certain extent, on the conditions before the cooler is activated (history effect). Parametric studies for some tests revealed that actually this dependence could be stronger than expected, and therefore the code simulations for Phase 4 could strongly depend on the correct simulation of the transient conditions before the cooler activation. This sensitivity to the correct initial conditions may pose a severe challenge to the codes when these are used to assess the cooler effect on the hydrogen distribution in a real containment.

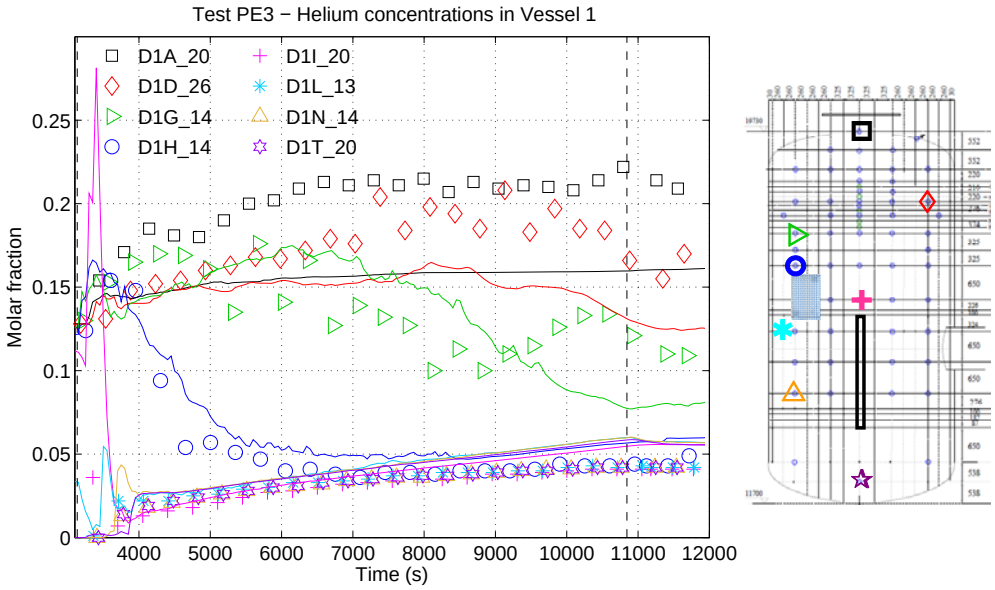

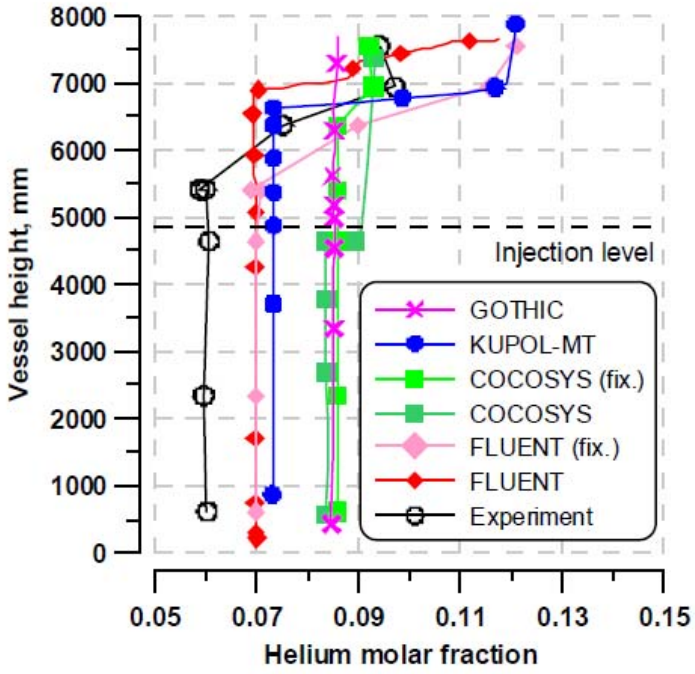

Figure 51: Helium concentrations calculated for (from top to bottom): PE3 test with GOTHIC [47] and S1 test with various codes [57].

Contrarily to the cooler, the spray activation has an overwhelming influence on the phenomena evolution. Therefore the correct prediction of the spray activation is less dependent on the containment conditions in the early phase of the accident scenarios (Phases 1 to 3).

In general, the de-pressurization rate in most of the transient stage was controlled by the steam condensed on the droplets, which is much larger than the vaporization from droplets, sump or liquid film on the wall. Since the heat/mass transfer models used by the codes are well established the initial depressurization was well captured by all codes (Figure 52), including LP codes. In the final period of the spray operation, however, pressure reduction due to condensation on droplets is partly compensated by the re-evaporation from the sump and heat transfer from the still hot walls. Under these conditions, the modelling of wall heat transfer and wall-to-liquid heat transfer on the sump becomes crucial for an accurate estimate of the final pressure. Therefore, in the post-test analysis, a large effort was dedicated to the proper representation of these two processes. In particular, in some simulations, enhanced turbulence due to the spray operation was assumed to justify large heat transfer rates and empiric solutions were proposed to represent sump water re-evaporation. Two-phase turbulence effects and radiative heat transfer to droplets, as well as mechanistic modelling of the sump could not be properly addressed. Nevertheless, this activity resulted in a substantial and generally valuable progress in the modelling of phenomena associated with spray operation, and therefore in the confidence to apply several codes to containment safety analysis.

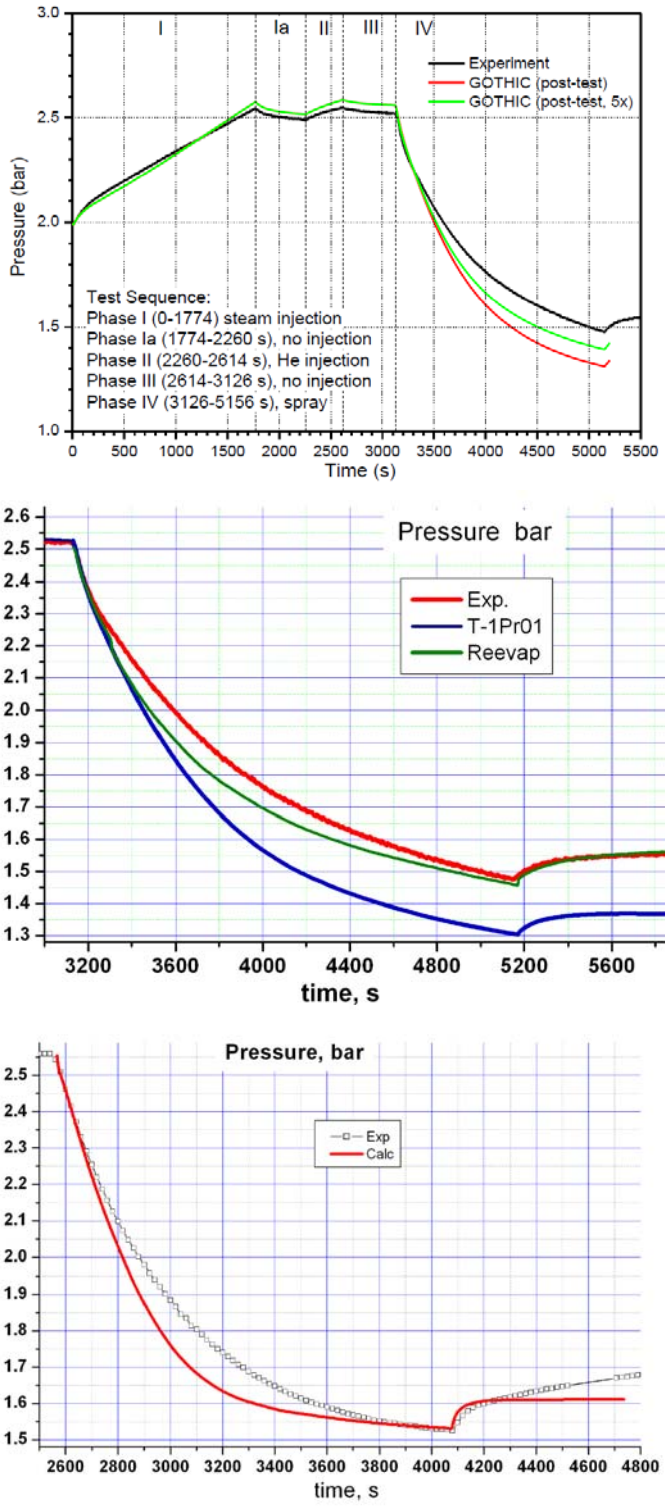

Figure 52: Pressure time evolution for (from top to bottom): PE1 test with GOTHIC [47] and FLUENT [53], and MERCO-1 test with FLUENT [53].

The gas species distribution below the spray nozzle elevation is generally well predicted (Figure 53), despite some specific effects in the transient state, which are not well captured.

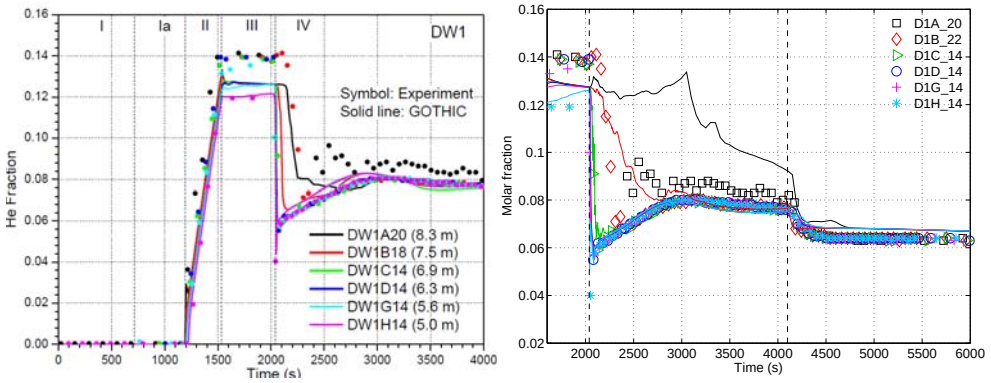
I
Ia
II
III
IV
DW1
Symbol: Experiment
Solid line: GOTHIC
DW1A20 (8.3 m)
DW1B18 (7.5 m)
DW1C14 (6.9 m)
DW1D14 (6.3 m)
DW1G14 (5.6 m)
DW1H14 (5.0 m)
He Fraction
Time (s)
Test PE2 − Helium concentrations in Vessel 1
D1A_20
D1B_22
D1C_14
D1D_14
D1G_14
D1H_14
Molar fraction
Time (s)

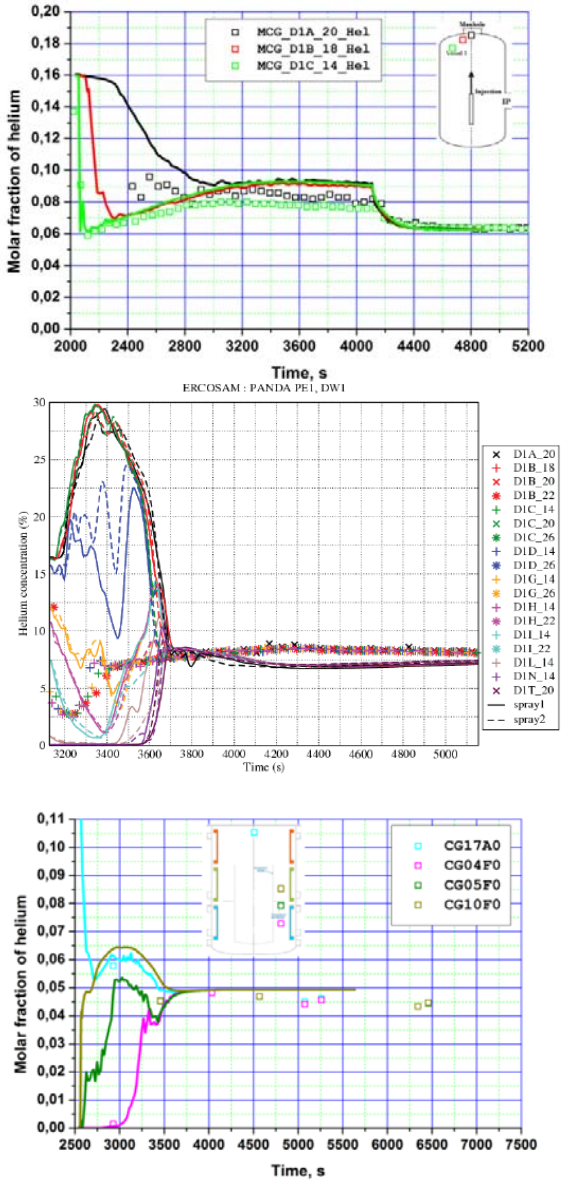

Figure 53: Helium gas concentrations calculated for (from top to bottom): PE2 test with GOTHIC ([44] and [47]) and FLUENT [53], PE1 test with ASTEC [48], and MERCO-1 test with FLUENT [53].

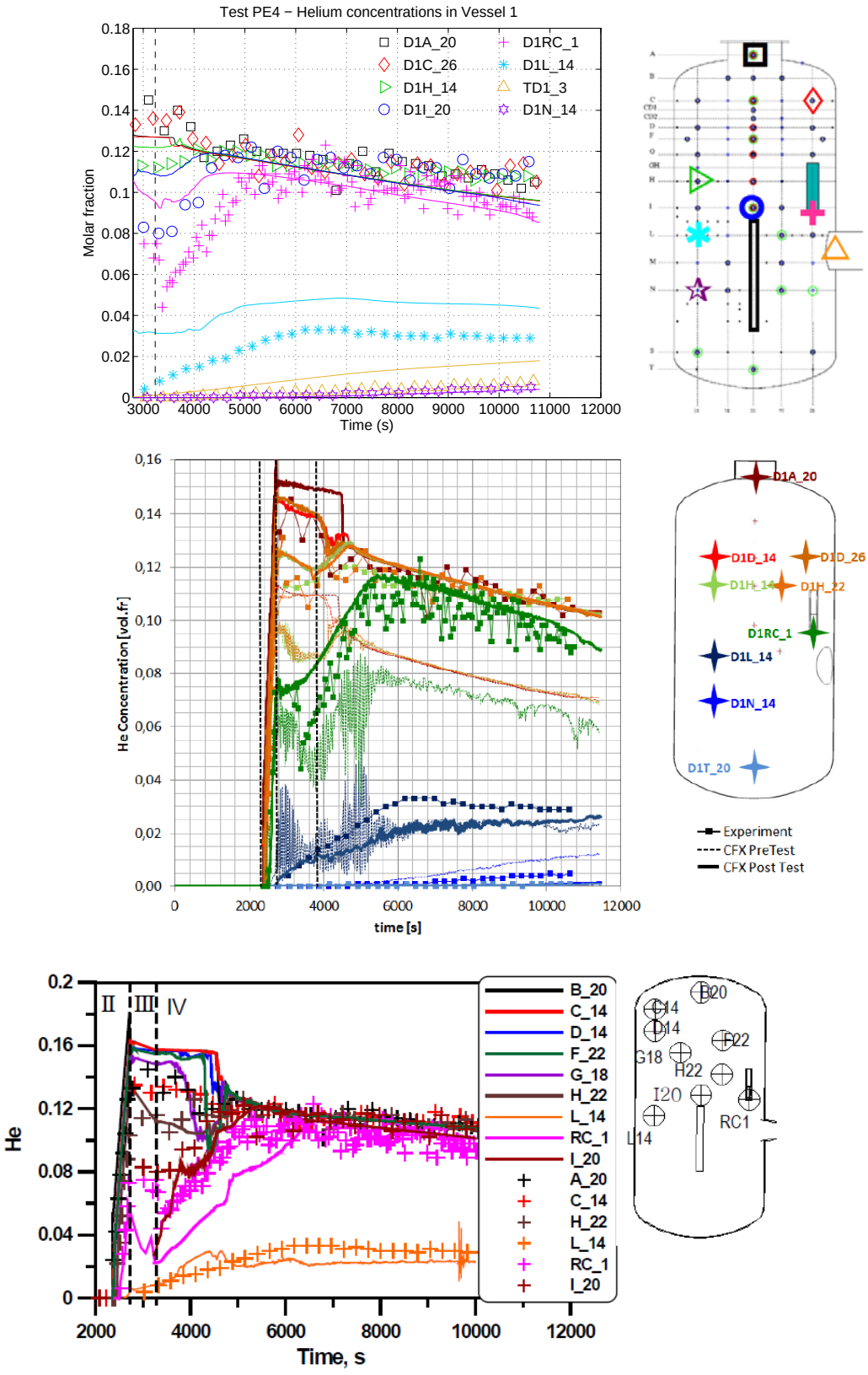

Figure 54: Helium concentrations calculated for PE4 test with (from top to bottom): GOTHIC [47], CFX [54] and FLUENT [47].

For the space above the spray nozzle, the simulations are generally much less accurate, with the prediction depending on a variety of modelling features and detail of the mesh (e.g. the two simulations with GOTHIC exhibit different trends for tests in PANDA). The large discrepancies observed in some local results (around the spray nozzle) with the only LP code (ASTEC) used for simulations of spray tests may indicate the difficulty to predict mixing with this type of codes, or simply a code-specific modelling/numerical issue. These results will be subject to further analyses. Although complete parametric studies could not be performed, for nearly all simulations the spatial distribution of the spray water injection (in simulations with CFD codes the spray angle) turned out to be a key parameter in the timing of the complete mixing.

For the heater tests (PANDA), nearly all simulations showed a good capability to reproduce the rather fast mixing above the heater inlet, and the very slow downward progression of the stratification front below this level (Figure 54). In this respect it is interesting to note that the heater effect is rather weak, and the quality of the simulations should be rated by comparing them with the calculation of a transient without the component.

This was only possible using the data in the MISTRA facility, where the MERCO-0 test (without heater) served as reference for observing the effect of the heater on the transient in MERCO-3 and MERCO-4 tests (Figure 55). For this test, the few CFD simulations addressing this issue were reasonably successful in predicting the genuine mixing effect of the heat source(s), which consists mainly in local differences but does affect little the global homogenization process. On the other hand, LP codes were less accurate in predicting mixing at various locations, mainly due to the difficulty to represent diffusion and convective motions behind the condensers. Another important finding (which confirmed results from previous projects) was that it is important to model the heat radiation from the heater to the wall structure and, for the case of MISTRA tests, flow transport behind the condenser driven by the heat loss sink, which played an important role in the helium distribution below the heater inlet.

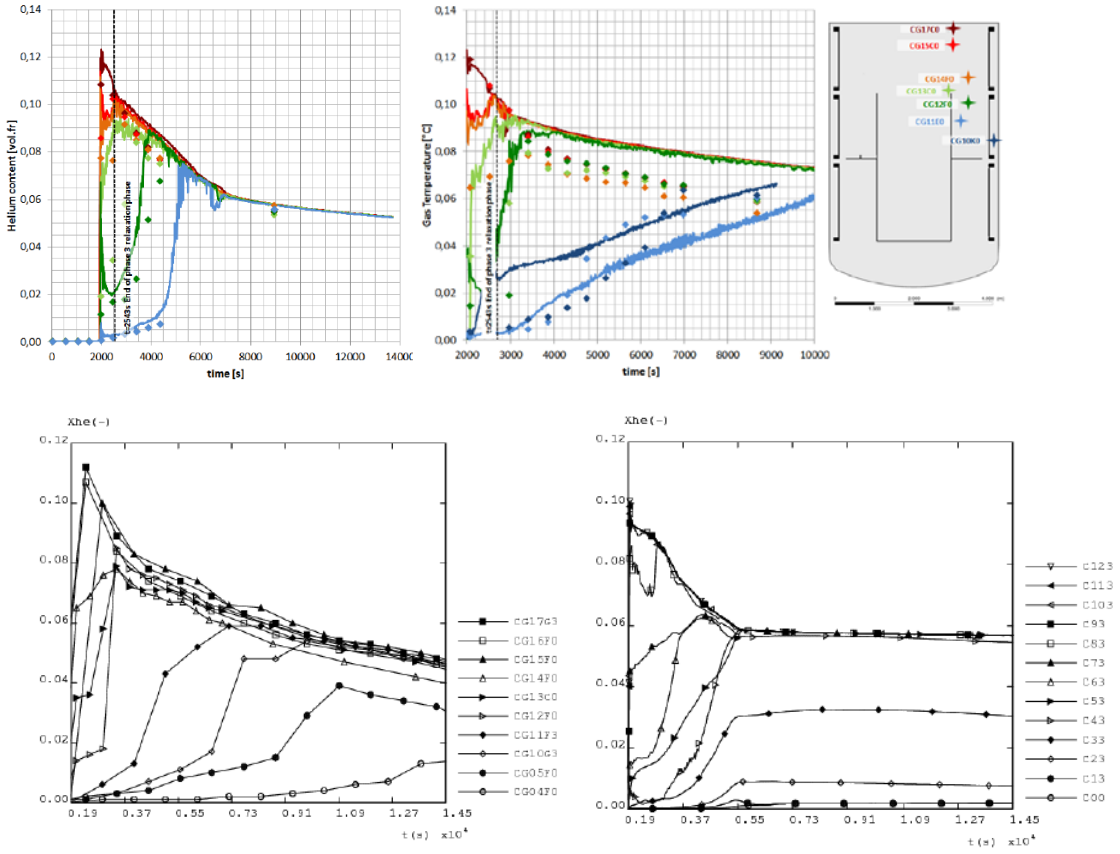

Figure 55: Comparison (top) between helium mixing in MERCO-0 test (without heater, left) and MERCO-3 test (with one heater, right) calculated with CFX [54], and (bottom) comparison between measured and calculated helium fraction at various locations calculated with TONUS [50].

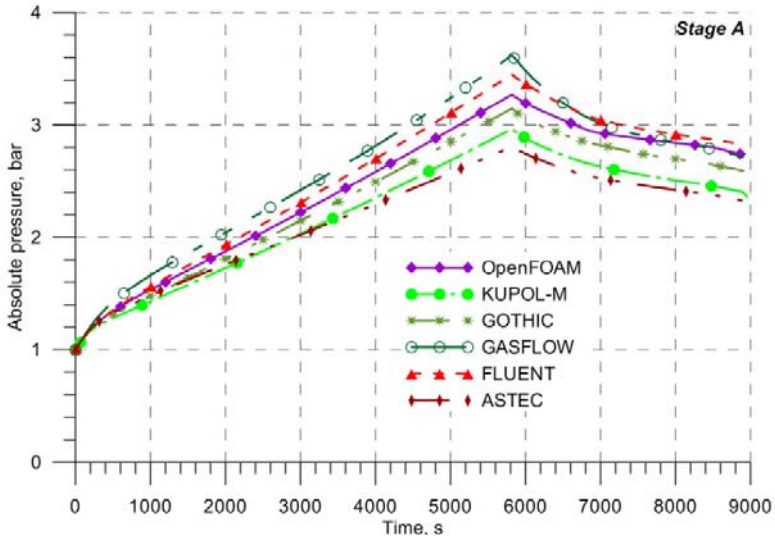

Figure 56: Pressure evolution during first three phases of K1 numerical benchmark calculated with various codes [45].

The two benchmarks based on the K1 and K2 analytical tests allowed code-to-code comparison at large scale (one order of magnitude larger than the facilities) and in a “blind-type” mode: e.g. not influenced by the knowledge of the experimental results. Since both LP and CFD codes were used for the analysis of K1 and K2, it has been possible to identify general differences on these two types of codes. For instance, in the calculation of the containment pressurization, the CFD codes tend to provide higher pressures because of higher calculated gas temperature due to gas compression and lower wall condensation (Figure 56).

With respect to hydrogen stratification build up in HYMIX K1 test (Figure 57), the LP codes predicted a more diffuse hydrogen distribution and therefore lower hydrogen concentration in the upper dome.

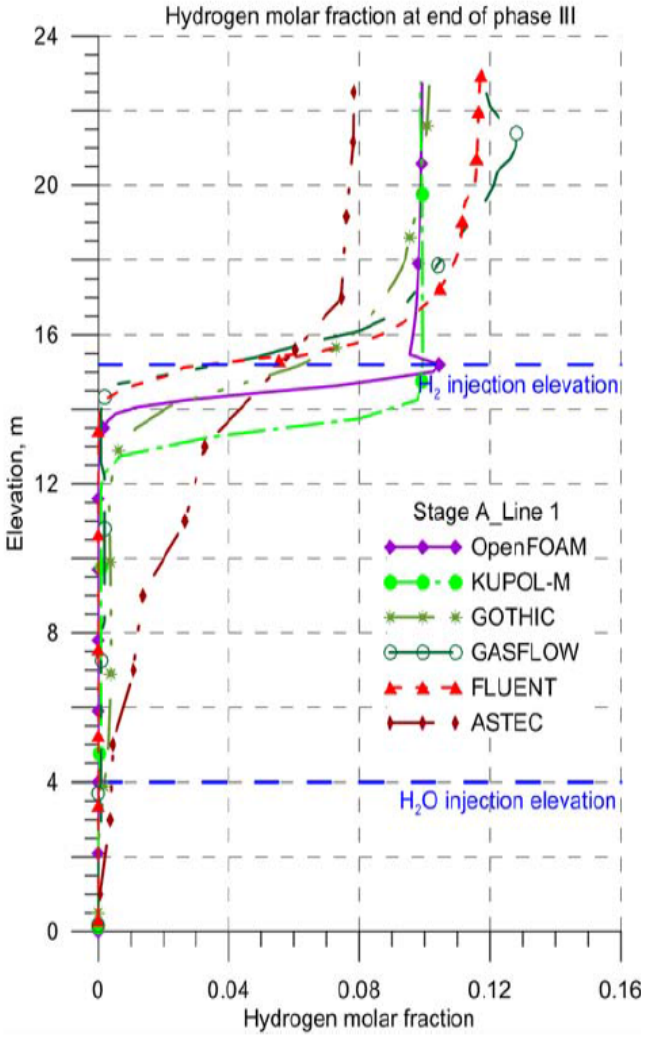

Figure 57: Hydrogen vertical distribution along Line L1 (axis) at the end of hydrogen injection in numerical benchmark HYMIX K1 calculated with various codes [45].

The depressurization rate during Phase 4 (spray operation) was similar in all calculations with the various codes (Figure 58), with notable differences, but without correlation between results and type of code.

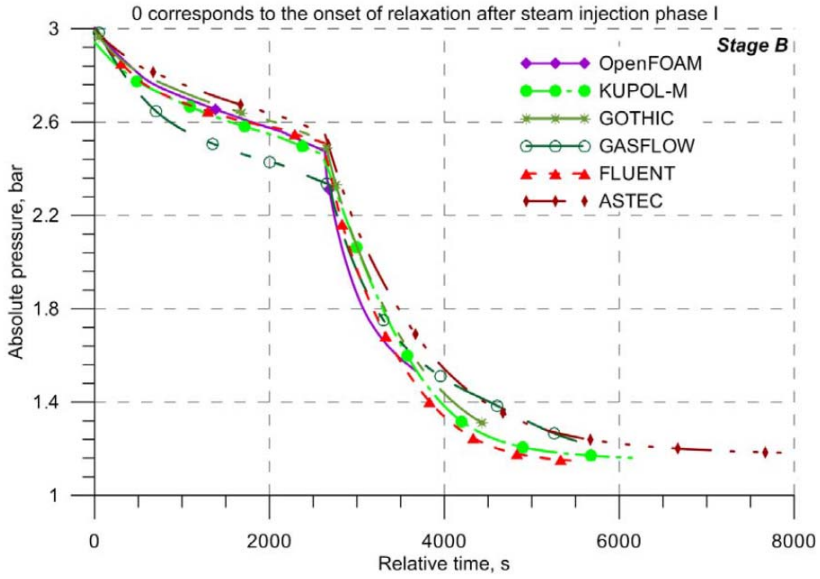

Figure 58: Depressurization in Phase 4 of numerical benchmark test HYMIX K1 calculated with various codes [45].

On the other hand, the simulated hydrogen concentration break-up by spray activation was faster with the CFD codes than that predicted using the LP codes (Figure 59, which shows the hydrogen concentration equalization at two positions). This result is consistent with the trend observed in the analysis of PANDA PE1 test.

Regarding test K2, featuring a compartmented geometry, the calculation of pressure build-up during the initial phase showed a spread between code simulations as in K1 test (Figure 61), with LP codes predicting higher condensation rates and thus slower pressurization. Differences between code predictions are also observed in the hydrogen distribution at the end of the stabilization phase (Figure 61) that originate from different assumptions about flow pattern in modeling with LP codes. The scattering in the hydrogen predictions in the hydrogen cloud is similar to that resulted in the analysis of SPOT and PANDA tests.

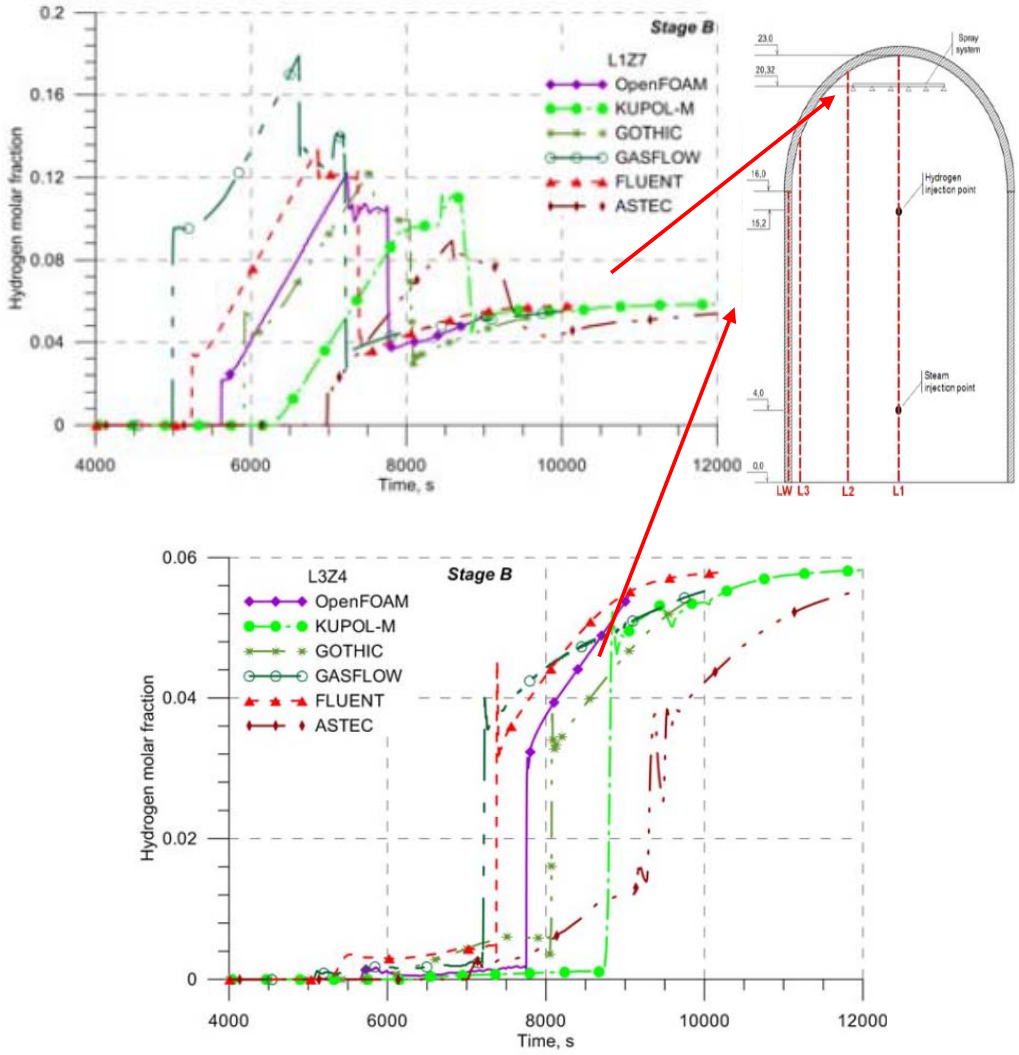

Figure 59: Hydrogen concentrations at two locations calculated for numerical benchmark test HYMIX K1 using various codes [45]

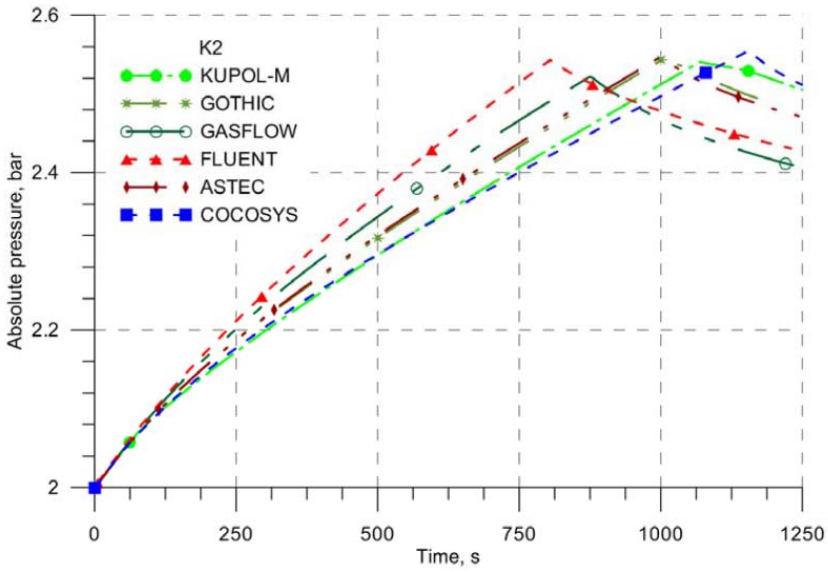

Figure 60: Pressure evolution during first phase of numerical benchmark test HYMIX K2 calculated with various codes [45]

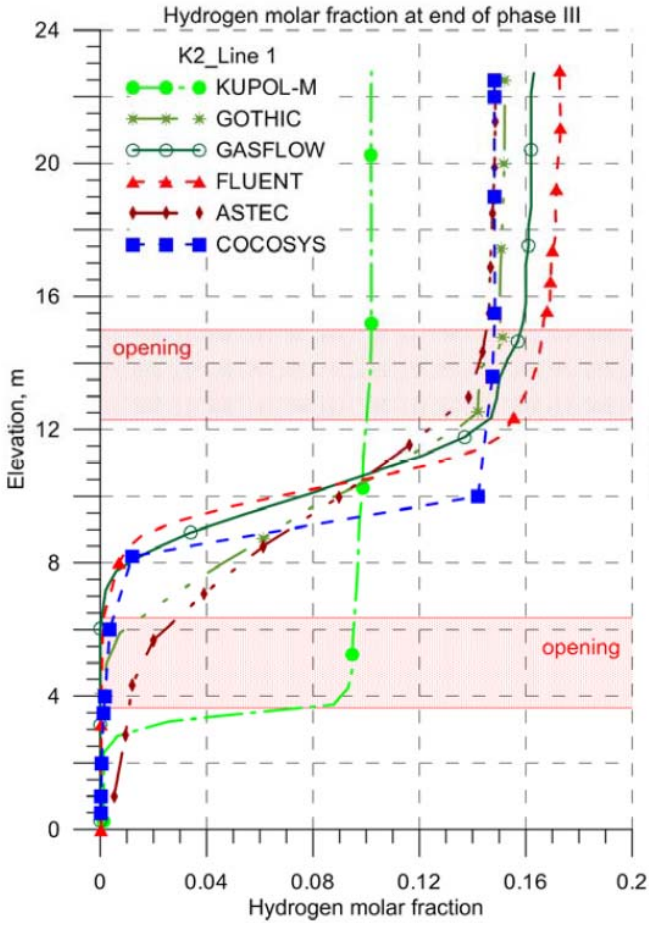

Figure 61: Vertical hydrogen distribution (along axis) calculated at the end of Phase 3 for numerical benchmark test HYMIX K2 with various codes [45]

Simulation of cooler activation in K2 test led to poor agreement between the code simulations with respect to cooler power and, therefore, depressurization (Figure 62). The primary reason of that is not sufficient calibration/verification of cooler model against SPOT tests (the verification resulted more time consuming that initially foreseen). Stratification break-up is predicted by all codes (Figure 63) although characteristic times do not match. Strong differences in code predictions are observed for hydrogen inter-compartment transport in dead-end volumes (Figure 64).

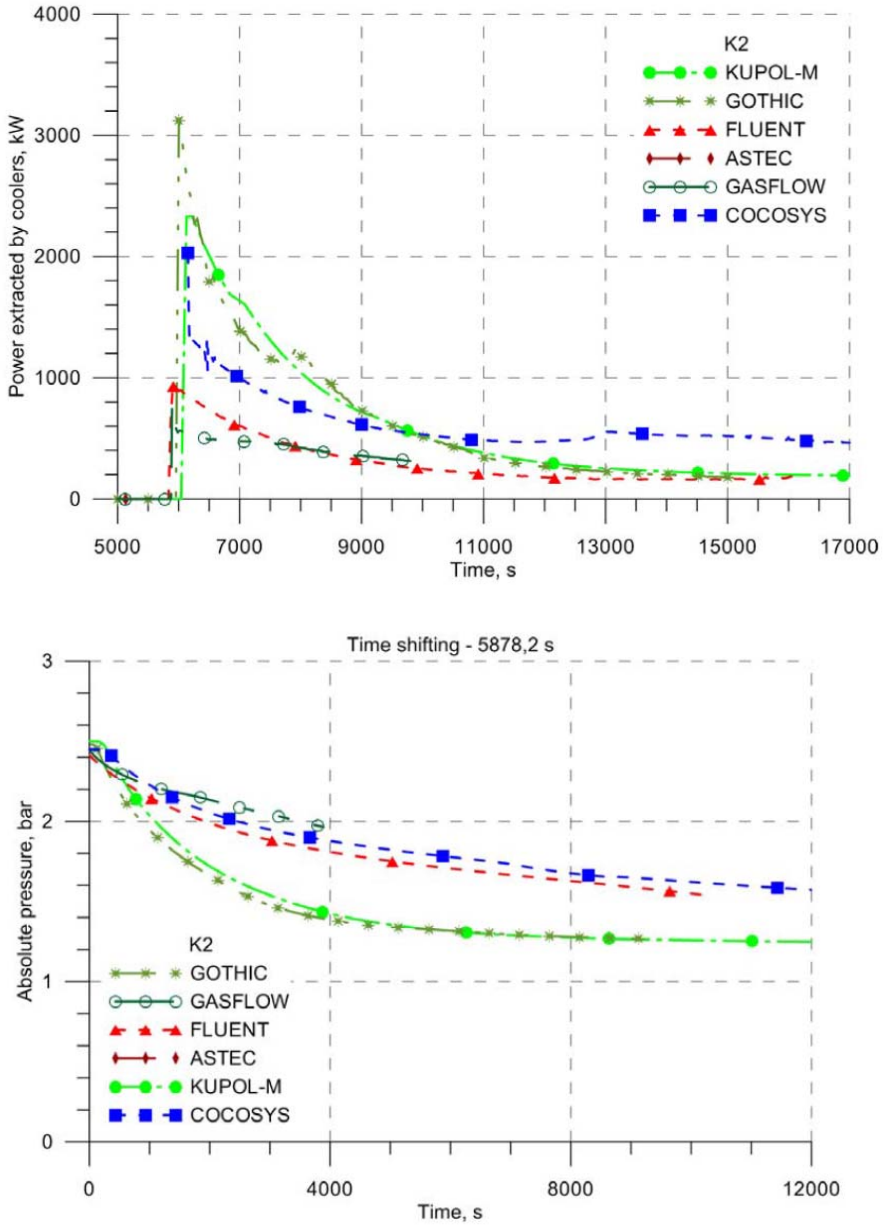

Figure 62: Cooler power (top) and pressure calculated for numerical benchmark test HYMIX K2 with various codes [45].

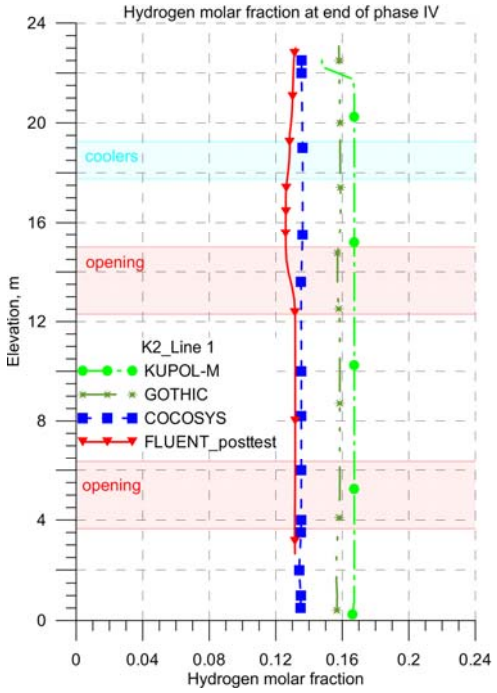

Figure 63: Vertical hydrogen distribution (along axis) calculated at the end of Phase 4 for numerical benchmark test HYMIX K2 with various codes [45]

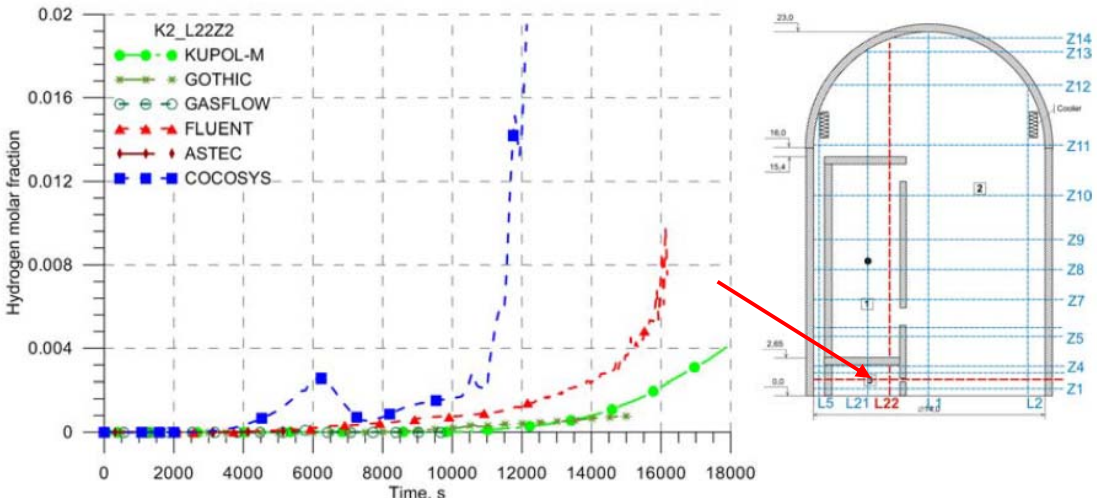

Figure 64: Hydrogen build-up during phase 4 of numerical benchmark test HYMIX K2 calculated with various codes [45]

The main outcome from K1 and K2 tests is that it is possible, using LP and CFD tools, to predict with reasonable accuracy/consistency most of the containment thermal-hydraulic phenomenology, including the effect of activation of safety systems studied in the ERCOSAM and SAMARA projects. Nonetheless, the results of simulations featured some degree of scattering. Further code validation activities including scalability of modelling choices, physics, SAMs, mesh needs (nodalization) remains to be investigated.

CONCLUSIONS AND RECOMMENDATIONS

The experimental and analytical investigations carried out within the EURATOM-ROSATOM ERCOSAM-SAMARA projects have contributed to the advancement of knowledge on issues that have relevance for reactor containment safety analysis.

The phenomenology addressed in TOSQAN, MISTRA, SPOT, PANDA tests and in the HYMIX analytical tests include pressurization, gas stratification build-up, stratification break-up, gas mixing, condensation, re-evaporation, de-pressurization under the effect of spray, cooler or heater activation. These phenomena are expected to take place in the containment of LWR/HWR during a postulated severe accident with core degradation and release of hydrogen.

The cooler and spray activation led both to containment de-pressurization. The de-pressurization rate was faster with the spray due to the high spray water mass injection flow rates and the drop-steam direct contact heat/mass transfer. The effect of spray activation on the gas species evolution was overwhelming, whereas the effect of the cooler was limited to the region below the cooler and immediately above the component. Due to the strong mixing effect of the spray, the analyses of these tests resulted less complicated than for the cooler tests, for which the fidelity of the simulation depends on the correct representation of various processes.

The heater tests, showed that the convection induced by the heat release has a mixing effect on the region above the heater inlet. The mixing below the heater inlet is controlled by slow processes (diffusion and thermal effects), and affected by the specific geometry of the containment. Moreover, the modeling of thermal radiation, although it was not critical for the prediction of the gas species evolution in the tests addressing only the thermal effects of the PARs, was important for accurately reproducing other variables, and should certainly be considered in full-scope simulations.

The experimental database obtained with the projects has already been used by the project Organizations to assess various computational tools and to advance modeling capabilities and simulation approaches. The two step approach (pre- and post-test analysis) resulted in a substantial and generally valuable progress in the modelling of phenomena associated with spray, cooler and heater operation, and therefore in the confidence to apply several codes to containment safety analysis.

A detailed description of the experiment phenomenology and of the test analysis has been reported by the project Organizations in the various project reports. Some of the project findings have been already published in various conferences [59-66] and a special session devoted to ERCOSAM-SAMARA is planned in ICAPP 2015 [67-74].

As follow-up of the ERCOSAM-SAMARA activities, the following general recommendations are outlined.

- The ERCOSAM-SAMARA approach to scale down from a generic scenario to experiments in various facilities and use the models validated with the facility data to analyze scenarios at large scale (HYMIX type) should be followed also in future projects intended to assess and validate advanced computational tools for nuclear safety analysis.

- The ERCOSAM-SAMARA experimental database should be further exploited and the project findings should be disseminated through scientific publications in conference proceedings and scientific journals
- The investigations on hydrogen risk should be continued, addressing more complex configurations and accident scenarios, more prototypical flow obstructions and compartments as well as different SAM component designs.
- The analytical activities associated with the tests should also aim for the improvement of numerical and physical models, especially for representing condensation/re-evaporation, turbulence, convective wall heat transfer in nearly stagnant regions, radiative heat transfer and the effects of spray on turbulence.
- Analytical tests (of type HYMIX) for code-to-code comparisons have to be carried out as blind type exercises for assessing the scalability of code simulations to scale approaching real LWR containments.

Acknowledgments

The ERCOSAM project (contract n° 249691) is co-financed by the European Commission within the 7th EURATOM Framework Programme on Nuclear Fission and Radiation Protection. The SAMARA project is co-financed by ROSATOM. This support is greatly acknowledged.

Without the continuous effort of the official delegates from the participant organizations, the project could not even completed successfully. The work of the following persons is deeply acknowledged.

Project coordination:

Irene Walthert, PSI

Tanja Hogg, PSI

SAMARA Management:

Arkady Kisselev, IBRAE RAN

Tatiana Yudina, IBRAE RAN

ERCOSAM Management team:

Salih Guentay, former PSI employees (now retired)

Ahmed Bentaib, IRSN

Michele Andreani, PSI

Isabelle Tkatschenko, CEA

Jerome Brinster, CEA

Frederic Dabbene, CEA

Jeanne Malet, IRSN

Project contributors:

Matt Krause, former AECL employees

Zhe (Rita) Liang, AECL

Podila Krishna, AECL

Danielle Abdo, CEA

Marie-Pierre Bohar, CEA

Jean-Luc Widloecher, CEA

Olivier Norvez, CEA

Etienne Studer, CEA

Hans-Josef Allelein, JUELICH

Ernst-Arndt Reinecke, JUELICH

Stephan Kelm, JUELICH

Michael Klauck, JUELICH

Wilfried Jahn, JUELICH
Lasse Götz, JUELICH
Rebekka Gehr, JUELICH
Alexandr Filippov, IBRAE RAN
Alexey Zaytsev, SSC RF-IPPE
Cataldo Caroli, IRSN
Alexandre Bleyer, IRSN
Nicolas Meynet, IRSN
Pascal Lemaitre, IRSN
Emmanuel Porcheron, IRSN
Sonia Benteboula, former IRSN employees
Thomas Jordan, KIT
Stefan Benz, former KIT employees
Zhanjie Xu, KIT
Christopher Boyd, US NRC
Ed M.G. Komen, NRG
Dirk Visser, NRG
Arne Siccarna, NRG
Mikhail Anatolyevitch Kamnev, JSC “Afrikantov OKBM”
Akhmir Muginovitch Khizbullin, JSC “Afrikantov OKBM”
Oleg Tyurikov, JSC “Afrikantov OKBM”
Martin Zimmermann, PSI
Horst-Michael Prasser, PSI-ETHZ
Max Fehlmann, PSI
Ralf Kapulla, PSI
Guillaume Mignot, PSI
Sidharth Paranjape, PSI
Medhat Sharabi, PSI
Simon Suter, PSI
Robert Zboray, PSI
Camille Ellen Zimmer, PSI
Joerg Dreier, PSI

European Commission:

Michel Hugon, former EC employees (now retired)
Roberto Passalacqua, EC

References

(ERCOSAM-SAMARA reports)

[1] S. Benteboula, A. Bentaib, J. Malet, A. Bleyer, “Scaling down analysis real NPP calculations to experimental facilities”. IRSN, D1.1 (2011-09), 2011.

[2] E. Porcheron, P. Lemaitre, A. Nuboer, “TOSQAN facility description”. P3.2 (2011-04), 2011.

[3] J. Brinster, I. Tkatschenko, J. L. Widloecher, “MISTRA facility description”. CEA, P3.3 (2011-03), 2011.

[4] N. Erkan, D. Paladino, G. Mignot, R. Zboray, R. Kapulla, M. Fehlmann, C. Wellauer, W. Bissels, “PANDA facility description”, PSI, P3.1 (2011-02), 2011.

[5] G. Mignot, R. Kapulla, D. Paladino, S. Paranjape, R. Zboray, M. Fehlmann,

W. Bissels, “Addenda to the facility description report of PANDA facility for ERCOSAM/SAMARA project’, P3.1B (2012-14/1), 2012

[6] M. Kamnev, A. Khizbullin, “SPOT facility description”, JSC “Afrikantov OKBM”, D5.11 (2012-09), 2012.

[7] A. Zaytsev, T. Popova, A. Philippov, A. Sorokin, T. Yudina, “HYMIX concept facility description”. IBRAE RAN, D5.5 (2013-21), 2013.

[8] C.Ledier, P. Lemaitre, A. Nuboer, E. Porcheron, “TOSQAN Test Protocols for 114 – 115 – 116 Tests”. IRSN, P3.5 (2012-07), 2012.

[9] D. Abdo, J. Brinster, F. Dabbenne, J.L. Windloecher, ”Test Protocol of MISTRA MERCO-0 Test, Phases I to III without SAM Activation”. CEA, P3.4_MERCO_0 (2012-6a), 2012

[10] D. Abdo, J. Brinster, F. Dabbene, J.L. Widloecher, “Test Protocol of MISTRA MERCO-1 Test: hollow cone spray test”. CEA, P3.4_MERCO_1 (2012-6b), 2012

[11] D. Abdo, J. Brinster, F. Dabbene, J.L. Widloecher, “Test Protocol of MISTRA MERCO-2 Test: middle condenser cooling test”. CEA, P3.4_MERCO_2 (2012-6c), 2012.

[12] D. Abdo, J. Brinster, F. Dabbene, O. Norvez, J.L. Windloecher, “Test Protocol of MISTRA MERCO_3 and MERCO_4 tests: Heater tests”. CEA, P3.4_MERCO_3&4 (2012-6c), 2012.

[13] M. Kamnev, A. Khizbullin, “SPOT test protocols”, JSC “Afrikantov OKBM”, D5.12 (2013-15), 2013.

[14] M. Kamnev, O. Tyurikov, “Test protocol for Test S1 (draft version)”. P3.13a (2013-01), JSC “Afrikantov OKBM”, P3.13a (2013-01), 2013.

[15] M. Kamnev, O. Tyurikov, “Test protocol for Test S2 (draft version)”. JSC “Afrikantov OKBM”, P3.13b (2013-02), 2013.

[16] G. Mignot, R. Kapulla, R. Zboray, M Fehlmann, C. Wellauer, W. Bissels, D. Paladino “Test protocol for PANDA Test PE1, hollow cone spray test“. PSI, P3.6A (2012-02), 2012.

[17] G. Mignot, R. Kapulla, R. Zboray, M Fehlmann, C. Wellauer, W. Bissels, D. Paladino “Test protocol for PANDA Test PE2, full cone spray test“. PSI, P3.6B (2012-10), 2012.

[18] G. Mignot, R. Kapulla, R. Zboray, M Fehlmann, C. Wellauer, W. Bissels, D. Paladino, “Test protocol for PANDA Test PE3, cooler test”. PSI, P3.6C (2012-11), 2012.

[19] G. Mignot, R. Kapulla, R. Zboray, M Fehlmann, C. Wellauer, W. Bissels, D. Paladino “Test protocol for PANDA Test PE4, heater test”. PSI, P3.6D (2012-01), 2012.

[20] G. Mignot, R. Kapulla, S. Paranjape, R. Zboray, M. Fehlmann, W. Bissels, D. Paladino, “Test protocol for test PE5, cooler test”. PSI, P3.6E (2012-16), 2012.

[21] A. Zaytsev, A. Lukyanov, T. Popova, “HYMIX benchmarking test protocol”. SSC RF-IPPE, D5.6 (2012-18), 2012.

[22] C. Ledier, P. Lemaitre, A. Nuboer, E. Porcheron, “TOSQAN test report, ERCOSAM tests 114, -115, -116”. IRSN P3.8 (2013-09), 2013.

[23] D. Abdo, J. Brinster, R. Tomassian, J. D. Wildloecher, “Quick Look Report for MISTRA MERCO_0-Steam (01/12/2011) and MERCO_0 (07/02/2012) and 13/4/2012) Tests”. CEA, P3.9A (2012-12), 2012.

[24] D. Abdo, J. Brinster, O. Norvez, J. D. Wildloecher, “Quick Look Report for MISTRA MERCO_1 Tests”. CEA, P3.9B (2012-12b), 2012.

[25] D. Abdo, J. Brinster, F. Dabbene, O. Norvez, J. D. Wildloecher, “Quick Look Report for MISTRA MERCO_2 Tests”. CEA, P3.9C (2012-12c), 2012.

[26] D. Abdo, J. Brinster, F. Dabbene, O. Norvez, JL. Widloecher, ”Quick-look report

for MISTRA MERCO_3 and MERCO_4 tests”. P3.9D (2013-18), 2013.

[27] D. Abdo, J. Brinster, F. Dabbene, O. Norvez, JL. Widloecher, “ Characterization

of Heater devices representatives, of a PAR before implementation inside the MISTRA facility”. CEA (2013-17), 2013

[28] M. Kamnev, “SPOT data analysis report”. JSC “Afrikantov OKBM”. P3.14 (2014-01), 2014.

[29] G. Mignot, R. Kapulla, S. Paranjape, R. Zboray, M. Fehlmann, W. Bissels, D. Paladino, “Test Report for Test PE1 – Hollow cone spray test”. PSI, P3.7A (2012-17), 2012.

[30] S. Paranjape, G. Mignot, R. Kapulla, R. Zboray, M. Fehlmann, W. Bissels, D. Paladino, “Test report for test PE2 full cone spray test”. PSI, P3.7B (2013-03), 2013.

[31] G. Mignot, S. Paranjape, R. Kapulla, R. Zboray, M. Fehlmann, W. Bissels, D. Paladino, “Test report for test PE3 cooler test with wall condensation”. PSI, P3.7C (2013-04), 2013.

[32] G. Mignot, R. Kapulla, D. Paladino, S. Paranjape, R. Zboray, M. Fehlmann, W. Bissels, “Test Report For Test PE4 Heat Source Test”. PSI, P3.7D (2012-13), 2012.

[33] R. Zboray, S. Paranjape, G. Mignot, R. Kapulla, M. Fehlmann, W. Bissels, D. Paladino, “Test report for test PE5 cooler test with wall condensation”. PSI, P3.7E (2013-05), 2013.

[34] N. Drobyshevsky, A. filippov, S. Grigoreyev, O. Tarasov, T. Yudina, “IBRAE RAN

Pre-test analysis report”. IBRAE RAN, P2.13 (2013-06) 2013.

[35] D. C. Visser, N. B. Sicarna, E. M. J. Komen, “ERCOSAM-WP2 pre-test report”. NRG, P2.5 (2013-07), 2013

[36] S. Benz, P. Royl, Z. Xu, T. Jordan, “Pre- and planning test calculations with GASFLOW”. KIT, P2.5 (2013-08), 2013.

[37] S. Kelm, W. Jahn, M. Klauck, L. Gotz, R. Gehr, „JUELICH Pre-Test Analysis

Report“. JUELICH, P2.17 (2013-10), 2013.

[38] R. Liang, ”AECL Planning and Pre-Test Analysis Report for the ERCOSAM-SAMARA projects”. AECL, P2.6 (2013-11), 2011.

[39] M. Andreani, “Planning and pre-test calculations for the ERCOSAM tests”. PSI, P2.1 (2013-12), 2013.

[40] F. Dabbene, “MERCO_0, MERCO_3 and MERCO_4 pre-test simulations”. CEA P2.2 (2013-13), 2013.

[41] M. Kamnev, O. Tyurikov, “JSC “Afrikantov OKBM” planning and pre-test analysis report”. JSC “Afrikantov OKBM”, P2.19 (2013-14), 2013.

[42] A. Zaytsev, A. Lukyanov, T. Popova, “Pre-test analysis report”. SSC RF-IPPE P2.14 (2013-19), 2013.

[43] T. Yudina, “IBRAE Report “HYMIX benchmarking tests”. IBRAE RAN, P4.1a (2013-16), 2013.

[44] R. Liang, “AECL Post-Test Analysis Report for the ERCOSAM-SAMARA Projects – Part I”. P2.12 (2014-02), 2014.

[45] A. Filippov, V. Tomashchik, T. Yudina, “HYMIX benchmarking tests: code-to-code comparison”. IBRAE RAN, P4.1 (2014-14), 2014.

[46] C. Boyd, “ERCOSAM WP2 post-test report”. US NRC P2.22 (2014-04), 2014.

[47] M. Andreani, M. Sharabi, “Post-test calculations for the ERCOSAM tests”. PSI P2.7 (2014-05), 2014.

[48] A.Bleyer, “ERCOSAM project: TOSQAN, PANDA and HYMIX post-tests analysis using ASTEC/CPA code”. IRSN, P2.8A (2014-06), 2014.

[49] J. Malet, “ERCOSAM project: CFD calculations of stratification and spray tests”. IRSN, P2.8B, 2014

[50] F. Dabbene, “MERCO_0, MERCO_3 and MERCO_4 post-test simulations”. CEA, P2.9 (2014-07), 2014.

[51] Z. Xu, “PANDA spray post-test simulations”. KIT, P2.10 (2014-08), 2014

[52] D. Visser, “ERCOSAM WP2 post-test report NRG”. NRG, P2.11 (2014-09), 2014.

[53] A.S. Filippov, S.Y. Grigoryev, O.V. Tarasov, T. A. Judina, “IBRAE RAN post-test Analysis report”. IBRAE RAN, P2.15 (2014-10), 2014.

[54] S. Kelm, M. Klauck, L. Goetz, R. Gehr, W. Jahn, “JUELICH Post-test analysis

report“. JUELICH, P2.18 (2014-12), 2014.

[55] M. Kamnev, O. Tyurikov, “ JSC “Afrikantov OKBM” post-test analysis report, Part I”. JSC “Afrikantov OKBM”, P2.20a (2014-13), 2014

[56] M. Kamnev, O. Tyurikov, A. Khizbullin, “JSC “Afrikantov OKBM” post-test analysis report, Part II”. “ JSC “Afrikantov OKBM, P2.20b (2014-13), 2014

[57] M. Kamnev, O. Tyurikov, A. Khizbullin, “SPOT code to data comparison”. “JSC “Afrikantov OKBM, P4.2 (2014-14), 2014

[58] J. Malet et al., “ERCOSAM WP4 Synthesis of tests and calculations activities”. IRSN, D4.1 (2014-29), 2014.

ERCOSAM-SAMARA publications (November 2014)

[59] D. Paladino, S. Guentay, M. Andreani, I. Tkatschenko, J. Brinster, F. Dabbene, S. Kelm, H.-J. Allelein, D.C. Visser, S. Benz, T. Jordan, Z. Liang, E. Porcheron, J. Malet, A. Bentaib, A. Kiselev, T.Yudina, A. Filippov, A. Khizbullin, M. Kamnev, A. Zaytsev0, A. Loukianov, "The EURATOM-ROSATOM ERCOSAM-SAMARA Projects on Containment Thermal-hydraulics of current and future LWRs for Severe Accident Management". Proceedings of ICAPP '12, Chicago, USA, June 24-28, 2012

[60] Z. Liang, M. Andreani, "Numerical Study on Interaction of Local Air Cooler with Stratified". Proceedings of ICAPP '12, Chicago, USA, June 24-28, 2012

[61] Z. Liang, M. Andreani, "Planning Calculations of Spray Tests for the ERCOSAM-SAMARA Project". 24th Nuclear Simulation Symposium, Ottawa, Ontario, Canada, 2012 October 14-16.

[62] S. Paranjape, R. Kapulla, G. Mignot, D. Paladino, R. Zboray, "Light Water Reactor Hollow Cone Containment Spray Performance Tests In The Presence of Light Non-condensable gas". The 15th International Topical Meeting on Nuclear Reactor Thermal Hydraulics (NURETH-15), May 12-16, 2013 Pisa (Italy)

[63] S. Paranjape, R. Kapulla, G. Mignot, D. Paladino, "Effect of thermal stratification

of thermal stratification on full cone spray performance in reactor containment for a scaled scenarios". ICONE 22, July 7-11, 2014, Prague, Czech Republic.

[64] A.S. Filippov, S.Y. Grigoryev, O.V. Tarasov, T.A. Yudina, "CFD Simulation Of PANDA and MISTRA Cooler Tests Of ERCOSAM-SAMARA Project". ICONE 22, July 7-11, 2014, Prague, Czech Republic.

[65] A. Filippov, S.Grigoryev, N. Drobyshevsky, A. Shyukin, T. Iudina, "CMFD simulation of ERCOSAM PANDA spray tests PE1 and PE2". CFD4NRS-5, Zurich 9-11 September 2014

[66] Grigoryev S.Yu., Filippov A.S., Shyukin A.A., Development and validation of condensation model for CFD investigations of NPP containment safety during a severe accident. Bull. Russ. Acad. Sci. Energetics, 4, P. 123-141, 2014 (in Russian)

ERCOSAM-SAMARA sessions in ICAPP2015:

[67] D. Paladino, A. Kiselev, "Main outcomes from the EUROATOM-ROSATOM ERCOSAM SAMARA parallel projects for hydrogen safety of LWR". Abs in: International Congress on Advances in Nuclear Power Plants (ICAPP 2015) May 3-6, Nice, France.

[68] A.S. Filippov, S.Y. Grigoryev, T.A. Yudina, A.E. Kisselev, O.V. Tarasov, "Complete CFD analysis of ERCOSAM-SAMARA exercises: a step toward advancing modeling of LWR containment under severe accident conditions". Abs in: International Congress on Advances in Nuclear Power Plants (ICAPP 2015) May 3-6, Nice, France.

[69] S. Benteboula, J. Malet, A. Bleyer, A. Bentaib, D. Paladino, S. Guentay, M. Andreani, I. Tkatschenko, J. Brister, F. Dabbene, S. Kelm, H.-J. Allelein, D.C. Visser, S. Benz, T. Jordan, Z. Liang, A. Kiselev, T. Yudina, A. Filippov, A. Khizbullin, M., Kamnev, A. Zaytsev, A. Loukianov, "EUROATOM-ROSATOM-ERCOSAM-SAMARA PROJECTS Scaling from Nuclear Power Plant to experiments". Abs in: International Congress on Advances in Nuclear Power Plants (ICAPP 2015) May 3-6, Nice, France.

[70] M. Andreani, M. Sharabi, A. Bleyer, J. Malet, F. Dabbene, D. Visser, S. Benz, Z. Xu, Z. Liang, S. Kelm, A. Filippov, A. Zaytsev, M. Kamnev, O. Tyurikov, C. Boyd, “Modelling of stratification and mixing of a gas mixture under the conditions of a severe accident with intervention of mitigation measures”. Abs in: International Congress on Advances in Nuclear Power Plants (ICAPP 2015) May 3-6, Nice, France.

[71] F. Dabbene, J. Brinster, E. Porcheron, G. Mignot, S. Paranjape, R. Kapulla, et al. “Experiemtnal activities on stratification and mixing of a gas mixture under the conditions of a severe accident with intervention of mitigation measures performed in the ERCOSAM-SAMARA project”. Abs in: International Congress on Advances in Nuclear Power Plants (ICAPP 2015) May 3-6, Nice, France.

[72] J. Malet, E. Porcheron, A. Bentaib, M. Andreani, G. Mignot, D. Paladino, S. Guentay, F. Dabbene, J. Brinster, D. Visser, Z. Xu, Z. Liang, S. Kelm, A. Kiselev, T. Yudina, A. Filippov, A. Zaytsev, M. Kamnev, C. Boyd, “Analysis of stratification and mixing of a gas mixture under severe accident conditions with intervention of mitigation measures”. Abs in: International Congress on Advances in Nuclear Power Plants (ICAPP 2015) May 3-6, Nice, France.

[73] M. Kamnev, O.Tyurikov, A. Khizbullin, A. Kiselev, T.Yudina, D. Paladino, M. Andreani, “Overview of SPOT experimental and analytical activities with KUPOL”. Abs in: International Congress on Advances in Nuclear Power Plants (ICAPP 2015) May 3-6, Nice, France.

[74] T.Yudina, A. Filippov, A. Kiselev, A. Bleyer, A. Bentaib, J. Malet, M. Andreani, D. Paladino, S. Guentay, R. Gehr, S. Kelm, H.-J. Allelein, S. Benz, T. Jordan, Z. Liang, T.Popova, “HYMIX benchmarking tests: code-to-code comparison”. Abs in: International Congress on Advances in Nuclear Power Plants (ICAPP 2015) May 3-6, Nice, France.